Surface Chemistry of Biodegradable Polymers for Drug Delivery Systems

Chang-Sik Ha[†] and Joseph A. Gardella, Jr.*,[‡]

Department of Polymer Science and Engineering, Pusan National University, Pusan 609-735, Korea, and Department of Chemistry, State University of New York at Buffalo, Buffalo, New York 14260-3000

Contents

* Corresponding author [fax (716) 645-3888; telephone (716) 645-2110; e-mail gardella@buffalo.edu].
[†] Pusan National University.
[‡] State University of New York at Buffalo.

1. Introduction

Impressive advances in biotechnology, bioengineering, and biomaterials with unique properties have led to increased interest in polymers and other novel materials in biological and biomedical research and development over the past two decades. Although biomaterials have already made an enormous impact in biomedical research and clinical practice, there is a need for better understanding of the surface and interfacial chemistry between tissue (or cells) and biomedical materials. This is because the detailed physicochemical events related to the biological response to the surface of materials still often remain obscure, even though surface properties are important determinants of biomedical material function.[1] In this regard, data available in the literature show the complexity of the interactions (surface reorganization, nonspecific/specific protein adsorption, and chemical reactions such as acid−base, ion pairing, ion exchange, hydrogen bonding, divalent-ion bridging) and the interrelationship between biological environments, interfacial properties, and surface functional groups responsible for the biological responses. Because of the multidisciplinary nature of surface and interfacial phenomena at the surface of biomedical polymers, there are several important issues that need to be addressed in the study of the interaction between the polymer material and the biological system at the surface.

Interfacial interactions are especially critical, and a polymer for biological systems, that is, a sort of biomaterial, must exhibit a specific surface chemical behavior in addition to the required bulk properties. A number of studies have been reported on (1) the characterization of the surface of the material under consideration in terms of its chemistry (elemental/molecular composition), physical morphology, and structure; (2) the interactions of macromolecules in the biological system with the characterized surface; and (3) the evaluation of the cellular response to the material by performing in vitro and in vivo experiments.[2−8]

Only limited work has been done, however, on the role of surface science in the surface reactivity to contribute to the understanding of materials in biological environments despite its significance.[2] Although many materials have been designed as biomaterials for active applications, a biodegradable polymer is one important application in which surface science techniques can have a clear and definitive role. Therefore, many studies have been published

Chang-Sik Ha received his B.S. degree in chemical engineering from Pusan National Universtiy, Korea, and his M.S. degree in chemical engineering from the Korea Advanced Institute of Science and Technology (KAIST), Seoul, Korea. He did graduate studies in polymer science at the KAIST, where he obtained his Ph.D. in 1987. He joined Pusan National University, Korea, in 1982, where he is currently a professor in the Department of Polymer Science and Engineering. His current research interests are hybrid organic–inorganic nanocomposites, biodegradable polymer blends and nanocomposites, periodic mesoporous organosilicas, organic electroluminescent devices, and nanostructured materials. He has two daughters (Jiwon and Jihyun) and one son (Jaehoon) with his wife Sheonja.

Joseph A. Gardella, Jr., received a B.S. degree in chemistry and a B.A. degree in philosophy from Oakland University in 1977. He received his Ph.D. degree in Analytical Chemistry from the University of Pittsburgh in 1981 after completing his thesis work in surface science and secondary ion mass spectrometry with Professor D. M. Hercules. In 1981, he carried out postdoctoral research at the University of Utah as a faculty intern for analytical development of FT-IR methods for surface analysis with Professor E. M. Eyring. In 1982, he joined the State University of New York at Buffalo, where he is currently a professor in the Department of Chemistry. His current research interests are analytical and surface chemistry and community-based environmental analysis. Away from his research works, Joseph also enjoys diverse community and public service activities as well as his family. He lives with his wife of 21 years, Carol, and their children, Claire Seung Hee and Joseph Jee Yoon.

on the bulk degradation behavior of degradable polymers.[9−12]

A few studies have been reported with regard to surface science for biodegradable polymers, but the main focus was on the investigation of the effect of surface modification of biodegradable polymers on the degradation behavior or on the effect of external materials such as biosurfactants on the surface properties of biomaterials.[13] For example, Jahangir reported on the influence of protein adsorption and surface-modifying macromolecules on the hydrolytic
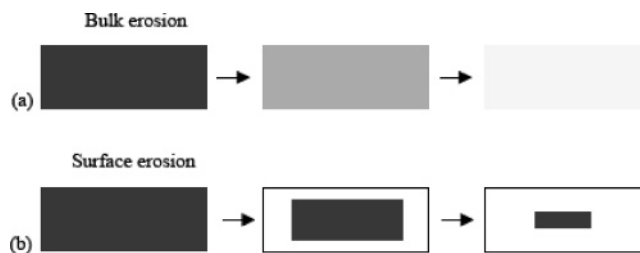

Figure 1. Schematic pictures of bulk erosion (a) and surface erosion (b). (Reprinted with permission from ref 14. Copyright 2004 Elsevier Science Ltd.)

degradation of a poly(ether-urethane) by cholesterol esterase.[13a]

The role of surface degradation processes versus bulk erosion is one of the most important issues. Degradation can proceed either in the bulk or at the surface of the material, as schematically drawn by Nam et al. in Figure 1.[14]

Depending on the pH conditions external and internal to a degradable polymer, either mechanism can dominate. In the case of bulk erosion, degradation proceeds throughout the polymer matrix and an immediate drop of molecular weight is observed, whereas the mass loss is retarded. In the case of surface erosion, the biodegradation proceeds exclusively at the surface.[15]

Studies of the surface of biodegradable polymeric materials[16−25] have provided chemical composition, structural information, or images of the morphological changes for visualization during hydrolytic degradation, but there have been few reports[22,25] of quantitative kinetic data from the surface degradation behavior. Thus, surface studies of the reactivity of biodegradable polymers have an essential value, not only for a fundamental understanding of hydrolytic surface degradation kinetics but also toward the design and formulation of new biodegradable polymers and their fabrication into new devices.[26]

An understanding of the bulk degradation is useful for applications such as degradable plastics for packaging. Surface degradation, however, is desirable in applications such as drug delivery systems. To maximize control over drug release, it is desirable for a system to degrade only from its surface. In systems with surface erosion, the drug release rate is proportional to the rate of erosion of the polymer. This eliminates the possibility of dose "dumping" (uncontrolled drug release) and facilitates device design.

Although some reviews have discussed a broad range of polymer surface characterization, even including surface reactivity of catalysts, none of them have dealt with biodegradation of polymers in terms of surface reactivity. In this paper, therefore, we review the role of the determination of surface reactivity as a means to contribute to the understanding of biodegradation kinetics and controlled drug release mechanism for some important biodegradable polymers such as poly(α-hydroxy acid)s, exemplified by poly(glycolic acid) and poly(lactic acid). Table 1 lists abbreviations of some important biodegradable polymers, which will be mentioned frequently in this review.

Table 1. Abbreviations of Some Important Biodegradable Polymers

abbreviation	full name
PLA	poly(lactide), poly(lactic acid)
PLLA	poly(L-lactide), poly(L-lactic acid)
PGA	poly(glycolide), poly(glycolic acid)
PDLLA	poly(DL-lactide)
PLGA	poly(DL-lactide-*co*-glycolide)
	poly(DL-lactic-*co*-glycolic acid)
	poly(L-lactide-*co*-glycolide)
	poly(L-lactic-*co*-glycolic acid)
PCL	poly(ϵ-caprolactone)
POE [poly-(ortho ester)]	3,9-diethylidene-2,4,8,10-tetraoxa-spiro[5,5]undecane-*co*-N-phenyl-diethanoamine (DETOSU/PDE)
P(3HB)	poly(*R*-3-hydroxybutyrate)
P(3HB-*co*-3HV)	poly(*R*-3-hydroxybutyrate-*co*-R-3-hydroxyvalerate)

2. Surface Quantitation of Biodegradable Polymers

2.1. Surface Chemistry: An Important Link to Properties

There is a general agreement that the ultimate performance of materials in many traditional and modern applications not only depends on their bulk properties but also relies heavily on their surface microstructure and interfacial behavior.[27] In this regard, surfaces play an important role in many technological processes, such as catalysis, corrosion, and adhesion. These processes depend on the chemical composition of the interface. Because the principal forces between molecules are van der Waals forces and they decrease with the seventh power of the intramolecular distance, the interaction between nearest neighbors is critical.[28] Therefore, the study of surfaces and surface phenomena on the atomic or molecular level defines modern surface science. The development of new catalysts, sensors, and ever smaller semiconductor-based devices, and so on, required understanding and characterization of surfaces on the molecular level, in turn, leading to the birth of new surface science-based technologies.[28] In today's world there are vast areas of materials technology that would benefit from the application of surface analysis techniques in both research and quality control.[29] In this sense, a large body of recent literature reviews and discusses a variety of important issues in the surface sciences of materials including biodegradable polymers.

In particular, the surface science of polymer materials has grown into a dynamic field, largely because of the application in such areas as composite materials, wetting, coatings, adhesion, friction, and biocompatibility.[30] Surface analysis of polymers can provide information about the chemical structure of both the polymer and surface active additives as well as surface contamination, which can impair the surface properties of many processes. Sometimes surface modifications are used to improve surface wettability and adhesion, and thus such modified surfaces are one of the main subjects of the surface analysis of polymers. The synthesis of new polymer materials, resulting in desired polymer-surface structures and composition, has also become more sophisticated and is driving the development of new spec-

troscopic probes and the continuing evolution of more established methods.[28]

Over the years an enormous number of techniques have been developed to probe different aspects of the physics and chemistry of polymer surfaces. In the next section, we will offer a brief overview of the current analytical tools for the surface characterization.

2.2. Surface Characterization Tools

2.2.1. X-ray Photoelectron Spectroscopy (XPS) and Secondary Ion Mass Spectrometry (SIMS)[31−37]

XPS, also called electron spectroscopy for chemical analysis (ESCA), has been the workhorse ultrahigh-vacuum (UHV) method for polymer applications. It provides chemical bonding information, exhibits high surface sensitivity, results in minor damage to the sample, and is relatively insensitive to the insulating properties of the sample.[31] A few reviews describe many types of information available from XPS measurements of polymers.[31−34] XPS is now routinely used to obtain the surface composition of polymers and to follow processing steps and degradation chemistry.[30]

Three aspects of XPS make it a desirable surface-analytical technique for polymers. Qualitative information from chemical shifts allows the identification of surface functionality in a polymer, quantitative analysis of the structure allows the determination of elemental and functional-group concentrations, and angle- and energy-dependent measurements allow this information to be determined for a depth profile, albeit with great difficulty due to the attenuation of signals from deeper depths.

Secondary ion mass spectrometry (SIMS) is another simple and very powerful surface analytical technique.[35−37] Mass analysis is commonly accomplished using quadrupole mass filters (QMF), time-of-flight (TOF), or magnetic sector mass analyzer. Instrumentally the development of TOF-SIMS is an area of great current interest, because TOF mass analysis gives the ability to detect ions of very high mass and therefore to analyze high molecular weight samples (10000−20000 amu). TOF-SIMS also has very low limits of detection due to the quasi-simultaneous detection of all masses. The SIMS experiment can be performed in one of two different modes—dynamic or static. In the majority of studies, static SIMS (SSIMS) has been used to provide the mass spectra of large, thermally labile organic compounds.[37a]

SIMS has several advantages over XPS such as the ability to detect all elements and their isotopic distributions, low detection limits, molecular secondary ions, and surface compositional sensitivity, but it also has major difficulties that limit routine analysis such as sample damage due to sputtering and a lack of understanding of the relationship between matrix-dependent secondary emission and surface composition. For more details on XPS and SIMS, readers should refer to the literature.[31−38]

Gardella and Hernandez de Gatica[2a] discussed the status and challenges of the use of surface chemical analysis based on XPS and SIMS for "biomaterials", that class of materials and their applications where the primary surface contact of a polymer, metal,

Table 2. Characteristics of Some Spectroscopic Techniques Suitable for Studying Polymeric Materials (Adapted from Reference 2c)

	XPS (ESCA)	IR and Raman	SIMS	ISS	HREELS
analysis environment	high vacuum	ambient	UHV	UHV	UHV
resolution	0.6 eV	-1 cm^{-1}	0.1$-$1 amu	variable	25$-$200 cm^{-1}
elemental/molecular information	no H detection/chemical shifts	???/functional group ID	all plus isotopes/MW molecules, fragmentation	no H or He/ resolution limited	functional group ID
detection limit	% of monolayer	% in volume 0.01 monolayer	ppm/ppb elemental, 0.01 monolayer molecular	% of monolayer	% of monolayer
lateral resolution	5 μm	-10 μm	10 nm (atomic) ??? molecular (ions)	none	none
depth sensitivity	>50 Å	μm range	10 Å?	3$-$5 Å	3$-$60 Å?
samples damage	small, sometimes with un-monochroma-tized X-rays	none	high (needs study), lower with static conditions	high (needs study)	none
major outcomes	elemental and chemical analysis, electronic structure	molecular vibrations, functional groups, bulk	low detection limits, molecular ions/fragmentation ion bonding	elemental, atomic orientation	surface-sensitive molecular vibrations

alloy, ceramic, or semiconductor, etc., is with a biological environment.[1,2] In that paper, they outlined the challenges of structure determination and the relationship with reactivity in these environments with some examples to describe areas for future growth of XPS and SIMS. These were highlighted by problems in the analysis of reactive materials, when the purpose of the material is not to be "inert" to the biological milieu.

2.2.2. Other Surface Characterization Techniques

In addition to XPS and SIMS, many other techniques have been used to characterize the surface properties of biomaterials.[38] Some of the techniques include contact angle methods, fluorescence spectroscopy, Auger electron spectroscopy (AES), and near-edge X-ray absorption fine structure (NEXAFS). More importantly, some other spectroscopic methods for surface analysis are also available including low-energy ion scattering spectroscopy (ISS) and high-resolution electron energy loss spectroscopy (HREELS) as well as Fourier transform infrared (FT-IR) [especially attenuated total reflectance (ATR)-FTIR], and Raman spectroscopy for vibrational spectroscopy at surfaces in addition to XPS and SIMS. Table 2 compares the analytical characteristics of some surface-sensitive spectroscopic measurements for biomaterials and polymers.[37a] As is well-known, FT-IR is useful as a bulk probe when utilized in the transmission, but sensitive to the near-surface region (1$-$5 μm), when ATR is employed.

When an ion beam impinges on a solid surface, several phenomena may occur. One such phenomenon is scattering of primary ions. This process is exploited by ISS to draw information on the outermost layers of solid samples. Due to its extreme surface sensitivity, ISS has been extensively applied in fundamental investigations of adsorption and desorption of suface layers, segregation in alloys, and surface reconstruction and in the characterization of applied materials, especially catalysts. Application of ISS to polymers has been developed following two main directions: investigation on the functional group orientation, using the shadowing effect, and detection of surface chemical composition and reactivity due to molecular orientation. ISS also has been used, in conjunction with other surface spectroscopies, to obtain depth profiles of multicomponent polymeric materials.[31]

On the other hand, HREELS is a technique that has been used extensively to prove small molecules adsorbed on single crystals and model catalytic systems. HREELS offers several advantages over optical techniques such as IR and Raman in that it has a single instrument vibrational and electronic spectral capability, high sensitivity (<0.1% of a monolayer), utility of application, that is, to various surface topographies, and perhaps the most useful feature—orientation sensitivity. If one considers a long-range dipole scattering mechanism to be operational in the HREELS, only normal vibrational modes that are orthogonal to the sample surface will be accessed by HREELS. This selection rule is analogous to that in IR reflection spectroscopy.[37b,c]

Table 3 shows a survey of examples of surface characterization of biomaterials-related systems using various techniques. For morphological features, some microscopic methods such as scanning electron microscopy (SEM), scanning tunneling microscopy (STM), and atomic force microscopy (AFM) have been also widely used. Each technique has its own strengths and weaknesses; usually a detailed characterization of the surface properties of a biomaterial typically requires the use of more than one method. Thus, there is no doubt that the multitechnique approach leads to information about the surface that is complementary in nature and provides a much broader picture than that given by one method alone.

In this review, however, we concentrate mainly on the utilization of XPS and SIMS for the surface chemistry of biodegradable polymers, because the two techniques have been proved to be quite useful for the analysis of their kinetic degradation behaviors as well as the quantitation of surface chemistry. Furthermore, they are the two most widely used UHV surface analysis techniques for biomaterials and biomedical devices, as can be seen in the literature survey (see Table 3). However, other surface analysis techniques such as AFM and surface wetting behavior are also mentioned, when necessary, in addition to the XPS and SIMS.

2.3. Surface Characterization of Biodegradable Polymers

A number of studies have been reported on the surface characterization of biomaterials and interfacial interaction between a polymer and a biological

Table 3. Survey of Examples of Surface Characterization of Biomaterials Related Systems Using Various Techniques Including XPS and TOF-SIMS

biomedical or biodegradable polymer systems	surface characterization	ref
bovine serum albumin upon adsorption to modified fluoropolymer substrates	fluorescence spectroscopy	Bekos et al.[56]
spacial control of neuronal cell attachment and differentiation on covalently patterned laminin oligopeptide on substrate	XPS	Ranieri et al.[57a]
titanium-alloys sterilized for biomedical applications	XPS, scanning auger micro-probe (SAM)	DeGatica et al.[58]
electrically charged polymeric substrates; to enhance nerve-fiber outgrowth in vitro	XPS, contact angle	Valentini et al.[59]
poly(L-lysine)-*graft*-poly(ethylene glycol) assembled monolayers on niobium oxide surfaces; a quantitative study of the influence of polymer interfacial architecture on resistance to protein adsorption	TOF-SIMS, optical waveguide light mode spectroscopy (OWSL)	Pasche et al.[60]
polymeric biomaterials	XPS, SIMS	Sabbatini and Zambonine[61]
angiotensin-converting enzyme−inhibitor from soy source	SIMS	Kinoshite et al.[62]
development of antimicrobial coatings for medical devices	XPS	Sodhi et al.[63]
biodegradable biomedical polyesters	XPS and SIMS	Davies et al.[16a]
biodegradable poly(anhydride) copolymers	TOF-SIMS	Davies et al.[16b]
biodegradable poly(ortho ester)s	XPS	Dematteis et al.[40]
biodegradable and -medical copolyester	XPS, TOF-SIMS	Lang et al.[41]
general discussion on the determination of structure and reactivity at the surfaces of materials used in biology by XPS and SIMS	XPS, SIMS	Gardella and deGatica[2]
biodegradable suture materials	XPS, SIMS	Brinen et al.[48]
modified PLA and PLGA films	XPS	Kiss et al.[49]
PLGA; quantifying the composition and determining the short-range order of the random copolymer	XPS and SSIMS	Shard et al.[51]
keratin fibers; application of cationic alkyl protein softener to bleached cashmere	TOF-SIMS	Volooj et al.[64]
adsorbed protein film; structure characterization; combined with principal component analysis (PCA)	TOF-SIMS	Xia et al.[65]
DNA sequencing	TOF-SIMS	Arlinghaus et al.[66]
review on SIMS microscopy for pharmacological studies in humans	SIMS, microscopy	Fragu and Kahn[67]
hyperbranched aliphatic polyester; probing their molecular weight on surfaces based on PCA	TOF-SIMS	Coullerz et al.[68]
phosphorylcholine functional biomimicking polymers; surface dynamic behavior	XPS, TOF-SIMS	Ruiz et al.[69]
cell adhesion to pluronic triblock copolymer; control surface peptide density while simultaneously preventing nonspecific protein adsorption	XPS, TOF-SIMS	Neff et al.[70]
biomimetic growth of apatite on hydrogen-implanted silicon; bioactivity of hydrogen-implanted silicon	SIMS, Rutherford back scattering (RBS)	Liu et al.[71]
protein resistance of PEG surface; ultrasensitive probing to test the resistance of PEG coating toward adsorption of lysozyme (LYS) and fibronectin (FN)	XPS, TOF-SIMS	Kingshott et al.[72]
multicomponent adsorbed protein films; with radiolabeling; discussion on the capabilities and limitations	XPS, TOF-SIMS	Wagner et al.[73]
hyaluronan and its sulfated derivative patterned with micrometric scale; surface microfabrication technique	TOF-SIMS	Barbucci et al.[74]
plasma-sprayed hydroxyapatite coating; characterization of chemical inhomogeneity	XPS, TOF-SIMS	Yan et al.[75]
nacre, known as mother-of-pearl; surface transformation to hydroxyapatite in phosphate buffer solution	XPS, SIMS	Ni and Ratner[76]
chemically and spatially controlled fibronectin and RGD substrates; neurite outgrowth on well-characterized surfaces	XPS, TOF-SIMS AFM, contact angle	Zhang et al.[77]
primary and immortalized cell adhesion characteristics to modified polymer surface: toward the goal of effective reepithelialization	XPS	Sigurdson et al.[78a]
biodegradable polymer formulations; tailored delivery of active keratinocyte growth factor from biodegradable polymer formulations	XPS	Cho et al.[55b]
biodegradable polymers; tools to rapidly produce and sceen biodegradable polymer and sol−gel-derived xerogel formulations	XPS	Cho et al.[55a]
cartilage for down-regulatation of growth factor expression in tracheal epithelium	SEM	Hicks et al.[78b]
binding of oligopeptides to cyclodextrins: "the role of the tyrosine group"	fluorescence spectroscopy	Bekos et al.[78c]
hierarchy of model systems for biomaterials interfaces: analysis	electron, ion and vibrational spectroscopies	Gardella[78d]
neuronal cell attachment to fluorinated ethylene propylene films with covalently immobilized laminen oligopeptides YIGSR and IKVAV	XPS	Ranieri et al.[57b]
synthesis and characterization of fluoropolymeric substrate with lithographically patterned minimal peptide sequences for cell adhesion studies	XPS, ATR-FTIR, TOF-SIMS, fluorescence spectroscopy	Vargo et al.[44b]
hydrogel polymer system; hydrated and dehydrated poly(hydroxy-ethyl methacrylate) (HEMA) based contact lens surfaces	XPS, SIMS	Schamberger et al.[79a,79d]
surface chemical studies of aging and solvent extraction effects on plasma treated polystyrene for cell culture applications	XPS, TOF-SIMS	Schamberger et al.[79b]
patterned neuronal attachment and outgrowth on surface modified, electrically charged fluoropolymeric substrates	XPS	Valentini et al.[80a]
surface chemical modifications of materials that influence animal cell adhesion—a review		Schamberger and Gardella[79c]
selective neuronal attachment to a covalently patterned monoamine on fluorinated ethylene propylene films	XPS, ATR-FTIR	Ranieri et al.[57c]
modification of surfaces designed for cell growth studies (book chapter)		Vargo and Gardella[44c]
novel supports for the development of high stability fiber optic-based immunoprobes	XPS	Litwiler et al.[81]
electrically charged tissue culture substrates enhance neurite outgrowth in vitro	XPS, contact angle	Valentini et al.[80b]
adsorbed protein film on mica and PTFE substrates	TOF-SIMS	Lhoest et al.[82]

**Table 4. Poly(β-hydroxy acids) under Investigation (Adapted from Reference 18)**

polymer	copolymer ratio			abbreviation
	benzyl β-malate	butyl β-malate	β-malic acid	
poly(benzyl β-malate)	100			$PMLABz_{100}$
poly(benzyl β-malate)-co-(butyl β-malate)	90	10		$PMLABz_{90}Bu_{10}$
poly(benzyl β-malate)-co-(butyl β-malate)	30	70		$PMLABz_{30}Bu_{70}$
poly(butyl β-malate)		100		$PMLABu_{100}$
poly(β-malic acid)-co-(butyl β-malate)		70	30	$PMLABH_{30}Bu_{70}$
poly(β-malic acid)-co-(butyl β-malate)		10	90	$PMLABH_{90}Bu_{10}$
poly(β-malic acid)			100	$PMLABH_{100}$
poly(benzyl β-malate)-co-(β-malic acid)	20		80	$PMLABz_{20}H_{80}$
poly(benzyl β-malate)-co-(β-malic acid)	80		20	$PMLABz_80H_{20}$
poly(benzyl β-malate)-co-(β-malic acid)	90		10	$PMLABz_{90}H_{10}$

Table 5. Theoretical and Experimental Values of Carbon Components in the C_{1s} Spectra of the Poly(β-hydroxy acids) (Adapted from Reference 18)

|	theor %					exptl %				
	1 C^1-C/C^1-H	2 C^2-CO_2	3 C^3-O	4 CO^4-CO_2	5 C^5-O_2	1 C^1-C/C^1-H	2 C^2-CO_2	3 C^3-O	4 CO^4-CO_2	5 C^5-O_2
$PMLABz_{100}$	54.5	9.1	9.1	9.1	18.2	54	9	9	9	16
$PMLABz_{90}Bu_{10}$	53.3	9.3	9.3	9.3	18.6	53	9	9	9	17
$PMLABz_{30}Bu_{70}$	43.8	11.2	11.3	11.2	22.4	46	11	11	11	20
$PMLABu_{100}$	37.5	12.5	12.5	12.5	25.0	37	13	13	13	24
$PMLAH_{30}Bu_{70}$	30.9	14.7	10.3	14.7	29.4	32	15	11	15	27
$PMLAH_{90}Bu_{10}$	6.8	22.7	2.3	22.7	45.4	9	23	3	23	43
$PMLAH_{100}$		25.0		25.0	50.0	17	23		23	37
$PMLABz_{20}H_{80}$	22.2	18.5	3.7	18.5	37.0	33	19	4	19	25
$PMLABz_{80}H_{20}$	50.0	10.4	8.3	10.4	18.9	48	11	8	11	19
$PMLABz_{90}H_{10}$	52.4	9.7	8.7	9.7	19.5	49	10	9	10	19

system. Several reviews and books have been published on this subject.[2-8]

With regard to the surface quantitation of biodegradable polymers, only limited works were published from the early works of Davies's group.[16] A single surface analysis method will rarely provide sufficient information to understand the surface chemical structure of a material completely.[3a] Thus, a multitechnique approach should be used, as it will yield pieces of information that can be integrated to provide a more complete picture of the surface. In this regard, both SIMS and XPS have been successfully used for the characterization of biodegradable polyesters. Here we show one example of how XPS and SIMS can be used to investigate the surface chemical structure of a synthetic biodegradable polymer, poly(β-malic acid), and its ester derivatives with the following general chemical structure:[18]
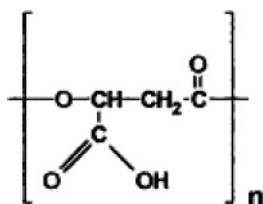

Poly(β-malic acid) ($PMLAH_{100}$), poly(benzyl β-malate) ($PMLABz_{100}$), poly(butyl β-malate) ($PMLABu_{100}$), and their copolymers with different copolymer ratios are listed in Table 4. Davies et al. analyzed XPS data based on C_{1s} spectra and O_{1s} spectra and found that the experimental and theoretical values for the carbon and oxygen components were in agreement with each other within the limits of experimental error, as shown in Table 5. For reference, Figure 2 shows C_{1s} spectra of the homopolymers with their structures.

They also carried out both positive and negative TOF-SIMS analysis. For instance, Figure 3 shows the negative ion TOF-SIMS spectra of the homopolymers (a) $PMLAH_{100}$, (b) $PMLABu_{100}$, and (c) $PMLABz_{100}$ in the range of m/z 100−230. In this mass region the negative ion TOF-SIMS spectrum of $PMLAH_{100}$ has two diagonostic ions at m/z 115 and 133. The ion at m/z 115 can be assigned to $[M_{PMLAH} - H]^-$, and the ion at m/z 133 can be assigned to $[M_{PMLAH} + OH]^-$, which have the structures below:
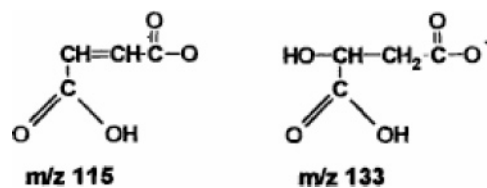
In a similar way, they could find fragment structures based on m/z as follows:
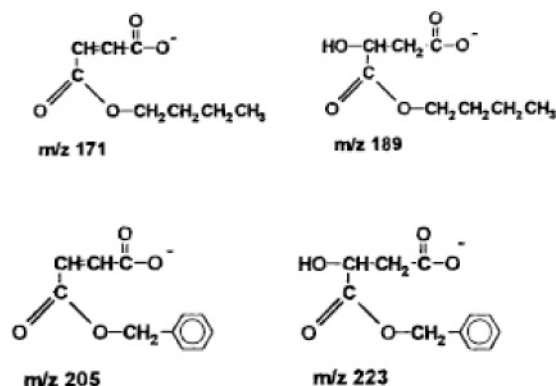
By definition, biodegradable polymers are "polymeric systems or devices which can be attacked by biological elements so that the integrity of the system
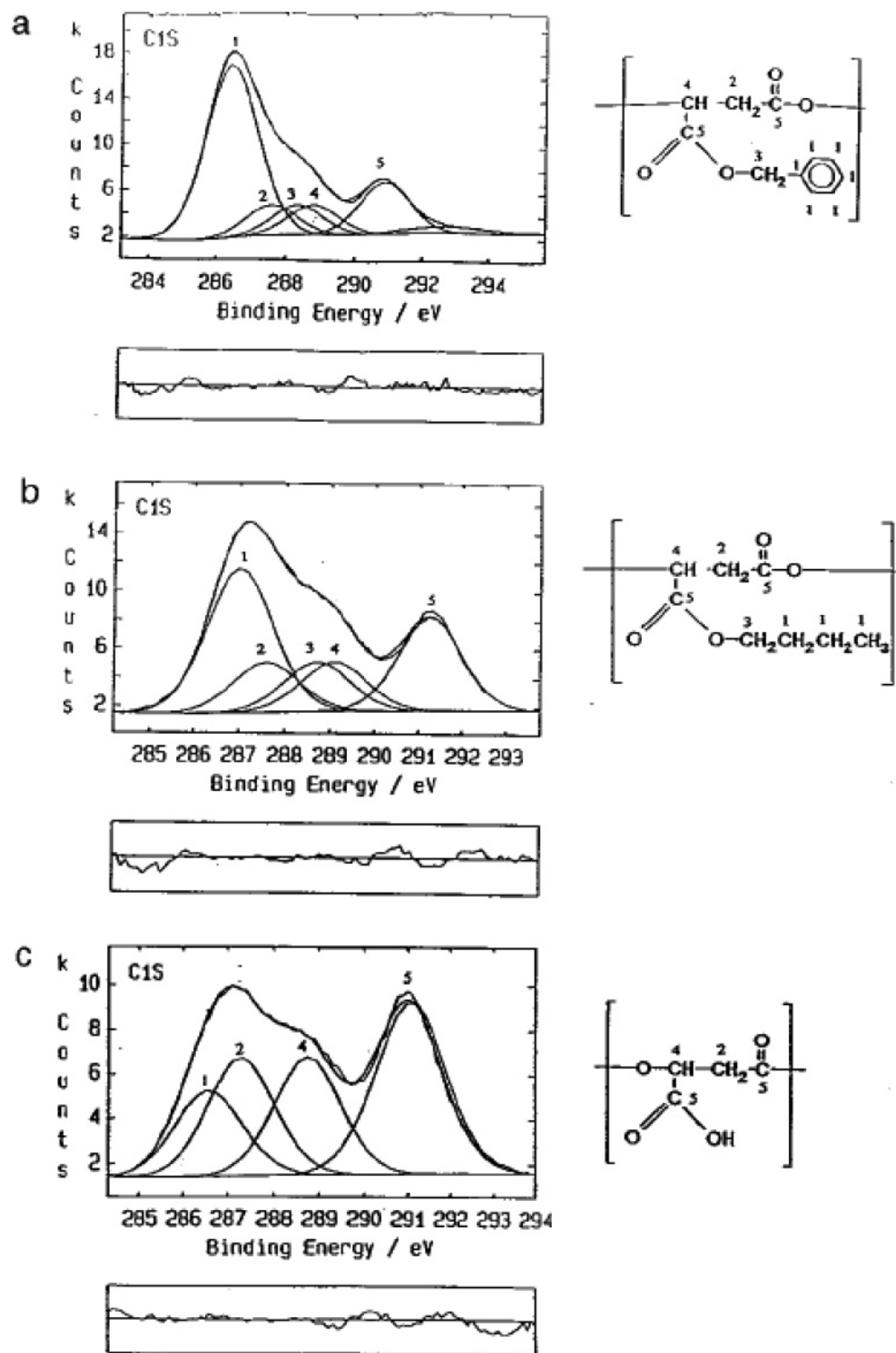
Figure 2. C_{1s} XPS spectra of the homopolymers: (a) $PMLABz_{100}$; (b) $PMLABu_{100}$; (c) $PMLAH_{100}$. (Reprinted with permission from ref 18. Copyright 1997 American Chemical Society.)

is affected and gives fragments or other degradation by-products".[39] Thus, such observation of characteristic fragmentation patterns on SIMS spectra in terms of m/z and the related structural analysis are helpful for further analysis of degradation kinetics, which will be discussed in section 4. Davies and co-workers also investigated the surface chemical structure of novel biodegradable poly(ortho esters) prepared from N-methyl- and N-phenyldiethanolamine (MDE and PDE), respectively, using high-resolution monochromated XPS.[40]

XPS and TOF-SIMS were also used to characterize bulk and surface properties of another important biodegradable copolymer produced from agricultural feedstocks by Lang et al.[41] The microbial polyester, poly[(R)-3-hydroxybutyrate] [P(3HB)], produced by microorganisms as carbon and energy reserves, has attracted much interest due to its biodegradability and biocompatibility.[10] A large number of research studies have been accomplished on the synthesis and characterization of microbial polyesters, and a few review articles on this subject are also available.[10]
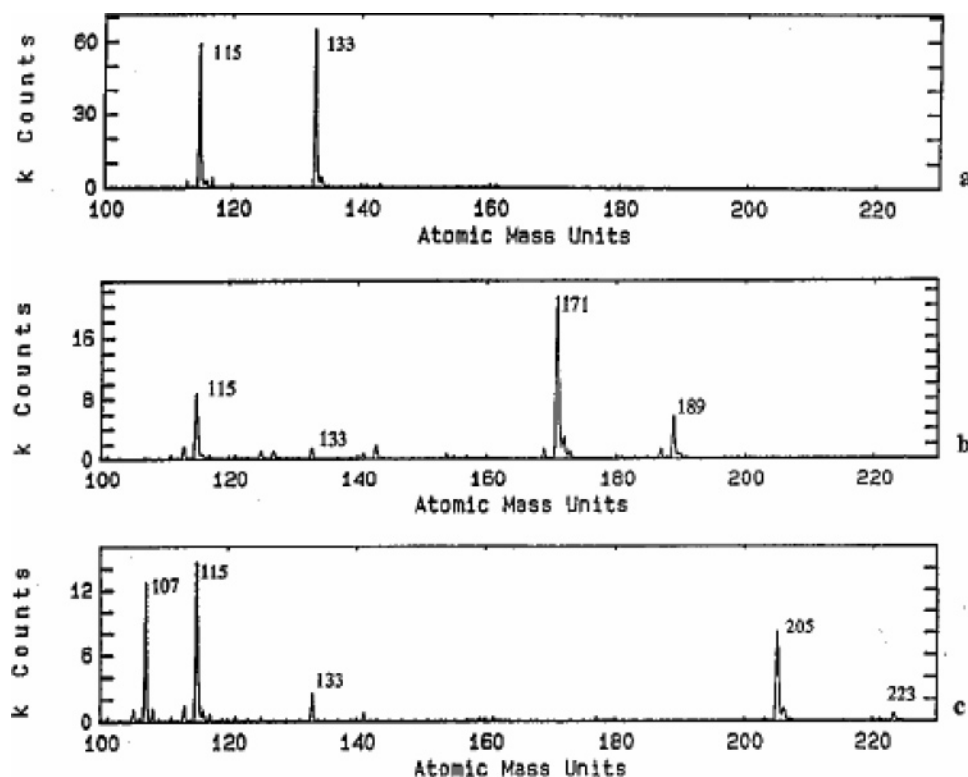
Figure 3. Negative ion TOF-SIMS spectra of the homopolymers (a) PMLAH$_{100}$, (b) PMLABu$_{100}$, and (c) PMLABz$_{100}$, *m/z* 100−230. (Reprinted with permission from ref 18. Copyright 1997 American Chemical Society.)

P(3HB) and poly[(*R*)-3-hydroxybutyrate-*co*-(*R*)-3-hydoxyvalerate] [P(3HB-*co*-3HV)] copolymers are two main microbial polyesters of today's interest presenting the advantages of biodegradability and biocompatibility over other thermoplastics with useful mechanical properties. Lang et al. analyzed P(3HB-*co*-3HV), a commercial product with the trademark Biopol, by multiple techniques including gas chromatography−mass spectrometry (GC-MS), nuclear magnetic resonance spectroscopy (NMR), and differential scanning calorimetry (DSC) as well as XPS and TOF-SIMS.[42] Table 6 summarizes negative mode SIMS data evaluated for quantification of the surface concentration c_s of butyrate (B) and valerate (V) based on Figure 4. Using the set of negative ion fragments, the mean surface stoichiometries from the c_s (percent) values were determined as c_s(B) = 89.0% and c_s(V) = 11.0% with a standard deviation of c_s(V) of 2.3%. These values are comparable to those estimated by ^{1}H NMR spectra and melting temperature data from DSC thermograms within the given errors. Moreover, XPS measurements confirmed the chemical composition of the Biopol surface, although the XPS data provided only a rough estimate of the surface composition contrary to TOF-SIMS measurements.

2.4. Surface Functionalization of Biodegradable Polymers

Although many materials, such as hydrolyzable polyesters and polyanhydrides, have been developed in the past decade to improve specific properties, such as biocompatibility, degradability, and drug delivery kinetics, there are still some limitations to their use. To overcome this, copolymers with functional side groups to modify the surface with biologically active moieties may be useful.[42,43] However, it may be difficult to control the density of surface functional groups such as hydroxyl or amine groups, due to the surface energy. Surface functionalization of fluorinated polymers was done using a radio frequency glow discharge plasma by Gardella and co-workers.[44] This surface modification can produce controlled densities of hydroxyl groups on the material surface, and then these groups provide sites for the covalent attachment of specific biomaterials such as proteins or peptides[45,46] and a new approach to controlling surface properties.

Biodegradable polyesters can be modified with various lengths of fluorocarbon (F-polyesters) end groups and arms as a new class of materials in terms of surface chemistry.[47] The design of the materials is based on principles of surface segregation of a component (in this case the end group) with the lower surface energy. It may be expected that F-polyesters may improve the controllable biodegradability at initial stages by controlling the surface composition of fluorocarbon groups. Cell adhesion may be controlled by adapting plasma and chemical modifications to these new fluorocarbon surfaces.[44b,c]

A series of fluorocarbon end-capped polyesters were synthesized by Lee et al. on the basis of the ring-open polymerization of lactones initiated by an alcohol.[47] The effect of fluorocarbon end group length on the surface structure of the F-polyesters before and after hydrolysis and its blend with polyesters was investigated by XPS. Angle-dependent XPS measurements showed that the dominant factors in defining the surface composition of F-polyesters are fluorocarbon chain length and molecular weight, not bulk composition. With a similar F/O ratio, a longer

Table 6. Major Negative Fragment Ions of P(3HB-*co*-3HV) Biopolyester[a] (Reprinted with Permission from Reference 41; Copyright 1998 American Chemical Society)

| 2 | | 1 | | | 0 | | Repetition units x negative ion structure | sum formula |
VB$_2$	B$_3$	V$_2$	VB	B$_2$	V	B		
		173	159	145	73	59		$M_{x+1}H(-CO)-$
255	241		169	155	-	69		$M_{x+1}(-RH)(-H)-$
255	241		169	155	83	69		$M_{x+1}(-OH)-$
257	243		171	157	-	71		$M_{x+1}(-R)-$
257	243		171	157	85	71		$M_{x+1}H(-O)-$
	257	199	185	171	99	85		$M_{x+1}(-H)-$
	259	201	187	173	101	87		$M_{x+1}H-$
		217	203	189	117	103		$M_{x+1}OH-$

[a] B and V denote the butyrate and the valerate monomer units, respectively. R is for the alkyl rest, which is either a methyl (B) or an ethyl (V).
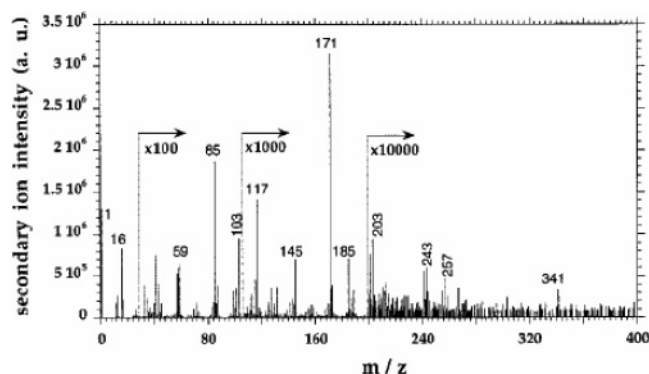

Figure 4. Negative mode SIMS spectrum (14 kV Cs$^+$) of the P(3HB-*co*-3HV) biopolyester. (Reprinted with permission from ref 41. Copyright 1998 American Chemical Society.)

fluorocarbon length gives a surface richer in fluorocarbon. These synthesized F-polyesters showed the property of retarded initial degradation rate dominated by the fluorocarbon chain chemistry, surface segregation, and water repellency. The surface modifications of F-polymers and their blends by plasma treatments were also investigated to give F-polymer surface reactivity with proteins or peptides.

Figure 5 shows the high-resolution C$_{1s}$ spectra of a typical F-polyester, F10C2-L-PLA14, film at various photoelectron takeoff angles. The C$_{1s}$ region measured at a takeoff angle of 90° showed contributions from C−O functional groups at 287.1 eV and from O=C−O at 289.1 eV from the PLA and from C−F$_2$ at 291.5 eV and from C−F$_3$ at 293 eV from the fluorocarbon. From the intensity of the C−F$_2$ fraction (from fluorocarbon) compared to that from O=C−O or C−O (from polyester), the intensity of this peak
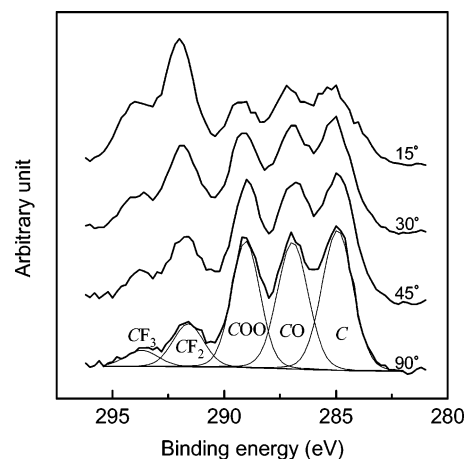
Figure 5. C$_{1s}$ spectra of F10C2−L-PLA14 at different takeoff angles. (Reprinted with permission from ref 47. Copyright 2001 American Chemical Society.)

increases gradually with increasing photoelectron takeoff angle. This suggests that the concentration of the fluorocarbon end group is much higher at the topmost surface than at the deeper regions.

Figure 6 is unit ratio profiles of various fluorocarbon end-capped polyesters obtained from angular-dependent XPS studies as shown in Figure 5. F-polyesters of two lengths [CF$_3$(CF$_2$)$_m$(CH$_2$)$_n$] were compared, where F7C1 and F10C2 represent $m = 6$ and $n = 1$ and $m = 9$ and $n = 2$, respectively, as the terminal end groups to L- and DL-polylactides (PLLA and PDLLA, respectively) and PLGA copolymers, shown in Scheme 1.

The concentration of fluorocarbon groups in F7C1−DL-PLA19 is higher than that of F10C2−L-PLA24,

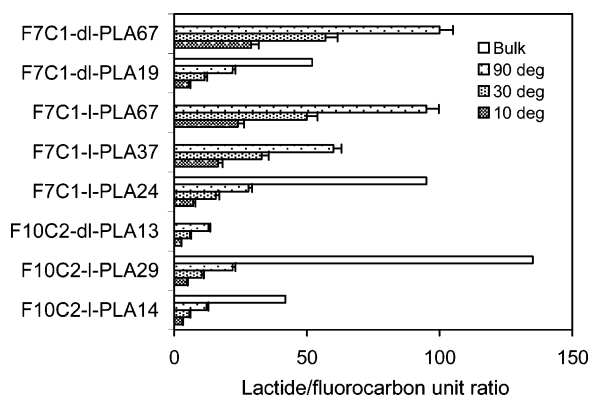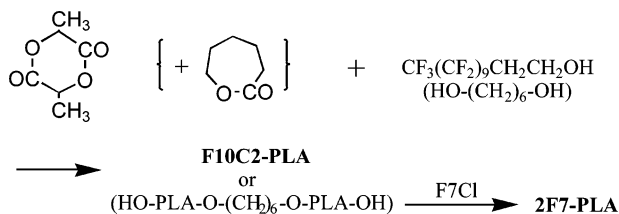**Figure 6.** Unit ratio profiles of various fluorocarbon end-capped polyesters. (Reprinted with permission from ref 47. Copyright 2001 American Chemical Society.)

Scheme 1. Synthesis of Fluorocarbon End-Capped Polyestes (Reprinted with Permission from Reference 47; Copyright 2001 American Chemical Society)

but angle-dependent XPS results are very similar to each other. This means that the longer the fluorocarbon group, the higher the surface fluorocarbon concentration, as expected; that is, the extent of surface segregation of the fluorocarbon group strongly depends on the length of fluorocarbon, as well as the bulk composition.

Brinen et al. used XPS and SIMS to examine the surface composition of copolymers of glycolide (cyclic dimer of glycolic acid) and trimethylene carbonate (TMC) as solvent-cast films. They found that XPS results on the polymers agreed with bulk composition data. SIMS measurements suggested surface enrichment of the TMC component.[48]

PLA and PLGA are biodegradable drug carriers of great importance, although successful pharmaceutical application requires adjustment of the surface properties of the polymeric drug delivery system to be compatible with the biological environment. For that reason, Kiss et al.[49] tried to reduce the original hydrophobicity of the PLA or PLGA surfaces by applying a hydrophilic polymer poly(ethylene oxide) (PEO) with the aim of improving the biocompatibility of the original polymer.[55] PEO-containing surfaces were prepared by incorporation of block copolymeric surfactants, PEO−poly(propylene oxide) (PPO)−PEO (Pluronic), into the hydrophobic surface. Films of polymer blends from PLA or PLGA (with lactic/glycolic acid ratios of 75:25 and 50:50) and from Pluronics (PE6800, PE6400, and PE6100) were obtained by the solvent-casting method, applying the Pluronics at different concentrations between 1 and 9.1% w/w. Wettability was measured to monitor the change in surface hydrophobicity, while XPS was applied to determine the composition and chemical structure of the polymer surface and its change with

surface modification. Substantial reduction of surface hydrophobicity was achieved on both the PLA homopolymer and the PLGA copolymers by blending the Pluronics at various concentrations. In accordance with the wettability changes, the accumulation of Pluronics in the surface layer was greatly affected by the initial hydrophobicity of the polymer, namely, by the lactide content of the copolymer. From the measurements of the water contact angles on PLGA copolymer surfaces modified with Pluronics at various concentrations, it was found that the hydrophobicity of the surfaces of the PLGA/Pluronics blend films decreased with decreasing lactide contents in the PLGA. The extent of surface modification was also found to be dependent on the type of blended Pluronics. The surface activity of the modifying Pluronic component was interpreted by using the solubility parameters.[49]

In a similar way, the surface chemistry of two series of PEO-containing PLLA matrix systems has been investigated using TOF-SIMS and XPS by Lee et al.[50] The two systems are (1) PLLA blend matrices with an amphiphilic Pluronic P104 surfactant and (2) PLLA-b-PEO diblock and PLLA-b-PEO-b-PLLA triblock copolymers. The phase separation was analyzed in determining the surface enrichment of the component and chemical composition at the polymer/air interface. For the blend system, the combination of the PPO component in the Pluronic surfactants drives the formation of a surface excess of Pluronic in the blends with PLLA. The surface excess profile showed a rapid increase in surface composition versus bulk composition for 1% Pluronic (bulk) to 5% Pluronic (bulk), but that profile leveled off from 5 to 50% Pluronic bulk. They found a rapid population of the topmost surface layer by the initial addition of Pluronic, followed by a more gradual increase likely due to increases in bulk distribution of Pluronic. They found that the PEO−PLLA block copolymer showed a surface excess of PLLA; these results are due to the better mixing of PEO and PLLA and the amphiphilicity of PEO as compared to the hydrophobicity of the PPO component of the Pluronic-based blend system. This is an unusual result in that a blend system would commonly show similar or more exaggerated surface excess of the same component, which illustrates the complexity of PEO-based formulations and surface chemistry.[50]

In addition to those works, many works on the surface characterization of other biomedical polymers including biodegradable polymers using XPS and TOF-SIMS have been reported.[51] In Table 3 one can see examples of surface characterization of biomedical polymers including biodegradable polymers using XPS and TOF-SIMS. Although poly(ϵ-caprolactone) (PCL) is also an important biodegradable polymer to show bulk erosion and has been used as a carrier in controlled release delivery systems,[52] no work on the role of surface chemistry of the PCL on the drug release behavior has yet been reported except a few studies on the surface modification of PCL for tissue engineering applications.[53] Poly(ethylene glycol) (PEG) or PEO and poly(L-glutamic acid) are also used for drug delivery systems,[54] but no work has been reported in terms of surface chemistry.

Table 7. Examples of Polymers Degraded by Hydrolysis in Vitro and in Vivo and Their Degradation Characteristics with Reference to Reference 15

biodegradable polymers	remarks	ref
poly(lactides), poly(glycolides) and others	synthetic biodegradable polymers as orthopedic devices	Middleton and Tipton[85]
biodegradable polyesters	medical and ecological applications	Ikada and Tsuji[86]
PLGA of various molecular weight served as a model compound	mechanisms of polymer degradation–mechanisms of polymer erosion	Gopferich[87a,b]
polyesters and polyamides	biodegradation of implantable polymers	Williams[88]
branched poly(DL-lactide-*co*-glycolide-D-glucose) and linear PLGA	factors influencing the release of peptides and proteins	Bodmer et al.[89]
polyesters and polyamides	biodegradability of synthetic polymers used for medical and pharmaceutical applications: principles of hydrolysis mechanisms	St. Pierre and Chiellini[90]
polyanhydrides	development of polyanhydrides as bioerodible polymers for drug delivery applications	Tamada and Langer[91]
poly(anhydrides)	biodegradation	Peppas and Langer[92]
poly(ortho ester)s	hydrolysis and erosion studies of autocatalyzed poly(ortho ester)s containing lactoyl-lactyl acid dimers; electrospray ionization/mass spectrometry (ESI/MS)	Schwach-Abdellaoui et al.[93]
poly(ortho ester)s	synthesis and erosion studies of self-catalyzed poly(ortho ester)s: hydrolysis; catalysis	Ng et al.[94]
poly(ortho ester)s	poly(ortho ester) biodegradable polymer systems	Heller and Himmelstein 95
PLGA (50:50) and poly[(50% ethyl glycinato) (50% *p*-methylphenoxy)-phosphazene] (PPHOS-EG50)	degradable polyphosphazene/poly(α-hydroxyester) blends: degradation studies.	Ambrosio et al.[96]
polyphosphazene	novel biodegradable polyphosphazenes containing glycine ethyl ester and benzyl ester of amino acethydroxamic acid (PGBP) as cosubstituents: syntheses, characterization and degradation properties	Qiu and Zhu[97]
novel thermosensitive poly(organo-phosphazenes) bearing methoxy-poly(ethylene glycol) (MPEG) and amino acid esters as substituents	syntheses, characterization and degradation properties	Song et al.[98]
polyphosphazene	novel biodegradable polyphosphazenes containing glycine ethyl ester and benzyl ester of amino acethydroxamic acid as cosubstituents: syntheses, characterization and degradation properties: synthesis and degradation behavior	Crommen et al.[99a,b]
polyphosphazene	histological evaluations of this particular polyphosphazene; controlled release using a new bioerodible poly-phosphazene matrix system	Laurencin et al.[100]
tyropsine-derived polycarbonate	surface characterization	PerezLuna et al.[101]

3. Drug Delivery from Biodegradable Polymers and Surface Chemistry

Polyesters, polyamides, poly(anhydrides), poly-(ortho esters), poly(phosphzenes), and many other synthetic polymers are degraded by hydrolysis in vitro and in vivo, and their degradation characteristics are well documented in the literature,[18] as shown in Table 7. PCL, PLA, and PLGA undergo autocatalyzed bulk hydrolysis.[79] Block copolymers of PLA or PLGA with PEG are also important biodegradable polymers, especially for drug delivery systems.[80,81] Thus, we discuss here some recent research relating to the application of biodegradable polymers for drug delivery systems in terms of surface chemistry.

3.1. Biodegradable Nanoparticles and Microparticles

Nanoparticles or microparticles as drug carrier systems are able to increase intracellular drug and gene delivery in vitro and in vivo to various tissues.[102–112] This has contributed to protection of drugs or DNA from degradation by the envelopment in or binding to a nanoparticle preparation. Additionally, nanoparticles seem to be well suited to traverse cellular membranes. Applications range from increasing the bioavailability of antiretroviral drugs,[102] over gene and oligonucleotide transfer,[106,113] to desensitization in peanut allergy.[108,114] Biodegradable nano-

particles have been used sometimes with electrically conductive polymers because electrical stimulation is capable of modifying cellular activities such as cell migration, cell adhesion, DNA synthesis, and protein secretion.[115]

Biodegradable nanoparticles or microparticles especially for PLGA,[116–118] or PDLLA, attract much interest for drug delivery systems.[115,119] The design of biodegradable nanoparticle or microparticle drug delivery systems with precisely tailored surface properties requires surface analytical methods that can relate polymer chemistry and fabrication parameters to the final surface chemistry of the nanoparticles or microparticles.

Shakesheff et al.[120] demonstrated using XPS that it is possible to identify significant variations in the surface chemistry of microparticles composed of PLA, PLGA, or block copolymers of PLA or PLGA with PEG.[88] They prepared two sizes of microparticles by a modified double-emulsion method. Their studies showed that XPS analysis provides a method of differentiating the presence of poly(vinyl alcohol) (PVA), PEG, and PLA–PLGA on microparticle surfaces. Estimates of the relative amounts of PLA, PLGA, PVA, and PEG monomer units at the microparticle surfaces based on curve-fitting analysis of the XPS data were presented.[120] For PLA and PLGA microparticles, relatively high surface contributions from PVA were evident. Comparison of the percentage areas of the carbon environments in the XPS data

enabled estimates of the surface contribution from vinyl alcohol and lactide/lactide-*co*-glycolide monomers to be calculated. For the block copolymers of PLA or PLGA with PEG segments, the presence of PEG at the polymer/water interface during microparticle formation reduced the requirement for PVA adsorption to achieve stabilization. This resulted in a decrease in the contribution of vinyl alcohol monomers from ~50% for the PLA−PLGA polymers to ~11% for the block copolymers.

Scholes et al. also determined surface levels of Poloxamer and PVA surfactant on biodegradable nanospheres using SSIMS and XPS.[121] The Poloxamers used here as stabilizers are Poloxamer 407 [weight-average molecular weight (M_w), 12600; PEO block length, 98 mol; PPO block length, 67 mol] and Poloxamine 908 (M_w, 25000; PEO block length, 122; PPO block length, 67 mol), of which structures are given below:

PEO-PPO-PEO (Poloxamer) copolymer

HO-[CH₂CH₂O]a-[CHCH₂O]b-[CH₂CH₂O]a-H
|
CH₃

Poloxamine copolymer

HO-[CH₂CH₂O]a-[CHCH₂O]b   [OCH₂CH]b-[OCH₂CH₂]a-H
| |
CH₃   CH₃
                NCH₂CH₂N
HO-[CH₂CH₂O]a-[CHCH₂O]b   [OCH₂CH]b-[OCH₂CH₂]a-H
| |
CH₃   CH₃

The nanospheres, which are of interest for site-specific drug delivery, were prepared using an emulsification−solvent evaporation technique with PVA. The surface chemical characterization of sub-200 nm PLGA nanospheres has been carried out using the complementary analytical techniques of SSIMS and XPS. The presence of surfactant molecules on the surface of cleaned biodegradable colloids was confirmed and identified on a qualitative molecular level (SSIMS) and from a quantitative elemental and functional group analysis (XPS) perspective. SSIMS and XPS data were also used in combination with electron microscopy to monitor the effectiveness of cleaning procedures in removing poorly bound surfactant molecules from the surface of nanospheres. The findings were discussed with respect to the development of nanoparticle delivery systems, particularly the composition of the surface for extending blood circulation times and achieving site-specific deposition.[121]

The double-emulsion method has been commonly used to make nanoparticles for drug delivery system.[122a,b] For instance, Zambaux at al. prepared and characterized nanoparticles of PLA and of blends of PLA and monomethoxypoly(ethylene glycol) by the double-emulsion method.[122b,123] In this review, many other drug delivery systems using nonbiodegradable polymer nanoparticles are not included, although such systems are also of continuing interest.[124]

3.2. Other Colloid Systems

Grassi et al. investigated[125] the potential of a sustained release formulation for paracetamol produced by melt pelletization. The chosen formulation was based on the combination of stearic acid as a melting binder and anhydrous lactose as a filler. After determination of the size distribution, the pellet was characterized by XPS as well as SEM, specific surface area, and true density determination. The in vitro release from every single size fraction (2000, 1250, 800, 630, <630 μm) was evaluated, and the release mechanism was analyzed with the help of an appropriate mathematical model. The results of drug content and superficial atomic composition were found to be constant in all pellet size fractions, attesting to the ability of melt pelletization in a high shear mixer to form a product with homogeneous composition. The mathematical model is built on the hypotheses that drug diffusion and solid drug dissolution in the release environment are the key phenomena affecting drug release kinetics. Smaller classes apart (particles are not perfectly spherical), the comparison between model best fitting and experimental data indicated that these hypotheses are reasonable. Moreover, model reliability was proved by the ability to predict drug release from a known mixture of the above-mentioned particle classes.

With respect to the surface eroding controlled drug delivery system, studies done by Davies and co-workers are noteworthy.[126,127] They recorded in situ AFM for the dynamic topographic changes occurring as a biodegradable polymer film, containing the protein bovine serum albumin (BSA), was eroded. An AFM was operated with the scanning probe immersed in an aqueous solution, allowing the surface morphology of these samples to be analyzed at the polymer/water interface. Control experiments demonstrated that the granular structure of the poly-(ortho ester) surface was roughened by the degradation process. The loss of protein particles embedded in a polymer film was then followed using the AFM. Analysis of the kinetics of the erosion process was undertaken using computational analysis of the three-dimensional AFM data, which enables volume changes occurring during the erosion to be quantified. These methods of volume analysis allow the comparative rates of protein and polymer loss from the eroding polymer surface to be assessed. Their data have implications for the design of surface-eroding controlled drug delivery devices and suggest a role for in situ AFM in the comprehension of the relationship between polymer biodegradation and protein release.[126]

Until recently, most of the previous studies relating to the surface characterization of biodegradable polymers used XPS together with other techniques including AFM and SEM. However, Davies and co-workers used SIMS as well as XPS to characterize polystyrene colloids with surface-grafted PEO as model systems for site-specfic drug delivery.[127]

A range of copolymer colloids with covalently attached PEO (2000 Da) chains were prepared by potassium persulfate-initiated emulsion copolymer-

Table 8. Elemental Compositions and C 1s Environments for Dialyzed PS−PEO 2000 Colloids from XPS Analysis, Assuming Homogeneous Layer throughout Region Sampled by XPS (Adapted with Permission from Ref 127; Copyright 1995 Elsevier Science Ltd.)

	% C	% O	% S	C−C/ C−H	C−O	CO_2	C−CO_2
PS	93.0	6.5	0.5	96	4		
PS−PEG2000a	92.4	7.6		92	8		
PS−PEG2000b	92.6	7.4		90	10		
PS−PEG2000c	90.1	9.9		85	15		
PS−PEG2000d	80.0	20.0		67	27	4	2
PS−PEG2000e	77.6	22.4		57	37	3	3
PS−PEG2000f	76.2	23.7	0.1	46	44	5	5

Table 9. Particle Sizes and Polydispersities of PS and PS−PEO2000 Colloids from PCS Analysis (Adapted with Permission from Ref 127; Copyright 1995 Elsevier Science Ltd.)

batch	mean size (nm)	polydispersity index
PS	184.2	0.072
PS−PEO2000a	155.3	0.028
PS−PEO2000b	140.5	0.048
PS−PEO2000c	101.5	0.066
PS−PEO2000d	81.8	0.045
PS−PEO2000e	66.9	0.091
PS−PEO2000f	62.6	0.050

ization of styrene with a PEO acrylate macromonomer. The surface orientation of the macromonomer chains has been confirmed by the complementary use of SSIMS and XPS. The detection of molecular ions diagnostic of PEG within the SSIMS spectra and their increase in relative intensity with increasing macromonomer content provided clear evidence of the surface presence of PEG for the range of PS−PEO colloids.
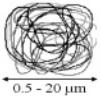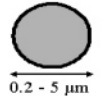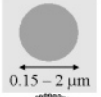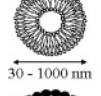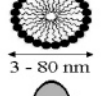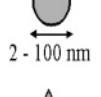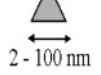
Similarly, the XPS studies showed that the level of PEO, as inferred from the ether C−O carbon environment within the C_{1s} spectra, increased with increasing levels of macromonomer in the latex, as shown in Table 8.

Table 8 shows the elemental composition of the surface layers of the PS latex, determined by XPS analysis, and the mean particle size and polydispersities of the PS−PEO2000 lattices are given in Table 9. The particle size of copolymer particles decreases as the quantity of macromonomer in the polymerization reaction is increased, where a proportional relationship is obtained between particle size and the molar ratio of PEO macromonomer in the polymerization reaction.

These surface analytical data on these near-monodispersed colloids were complemented by particle size, electrophoretic mobility, and colloid stability analysis, all of which showed a marked dependence on the level of surface PEO. The relevance of these findings is discussed both in terms of the particle formation mechanism and in the context of the potential of these colloids as model systems for proving the influence of PEO surface density on colloidal biodistribution in vivo.

The most commonly used colloid particle-based delivery systems are summarized in Table 10 with their typical average dimensions. In addition to more traditional particulate delivery systems, a variety of other nanomaterials have been developed more recently, such as quantum dots and nanocrystals, and their aqueous dispersions are considered as colloids due to their dimensions and surface properties. Various ways of delivering therapeutic agents with colloidal delivery systems were recently reviewed by Kostarelos.[128]

Table 10. Delivery System Types, Common Delivery from Each Type, and Most Widespread Biomedical and Pharmaceutical Uses (Reprinted with Permission from Ref 128; Copyright 2003 Elsevier Science Ltd.)

Delivery system and typical mean particle diameter	Representative system of each type	Characteristic applications
macrospheres hydrogels 0.5 - 20 μm	Alginate, gelatin, chitosan, PLGA microspheres synthetic, biodegradable, polymer hydrogels	• sustained release of therapeutics • scaffolds for cell delivery in tissue engineering
microparticles 0.2 - 5 μm	Polystyrene, microspheres	Targeted delivery of therapeutics
emulsions, microemulsions 0.15 – 2 μm	o/w, w/o/w, lipid, emulsions o/w microemulsions	Controlled and targeted delivery of therapeutics
liposomes 30 - 1000 nm	Phospholid and polymer-based bilayer vesicles	Targeted delivery of therapeutics
micelles 3 - 80 nm	Natural and synthetic surfactant micelles	Targeted delivery of therapeutics
nanoparticles 2 - 100 nm	Lipid, polymer, inorganic nanoparticles	• Targeted delivery of therapeutics • in vivo navigation devices
nanocrystals 2 - 100 nm	Quantum dots	Imaging agents

4. Surface Degradation: Kinetic Aspects

In Table 7, we showed some important biodegradable polymers, which are degraded by hydrolysis in vitro and in vivo. Similarly, PCL, PLA, and PLGA undergo autocatalyzed bulk hydrolysis.[84] Polymers derived from carbonic acid are sometimes degraded by oxidation in vivo.[129,130] Microbial polyesters such P(3HB) or P(3HB-co-3HV) are degraded by enzymatic attack. First, we discuss enzymatic biodegradation in terms of surface chemistry followed by the hydrolytic biodegradation.

4.1. Surface Chemistry of Enzymatic Biodegradation of Microbial Polyesters

One of the recent trends of biodegradable polymer research is focused on the desired life span. Because the mechanical properties of microbial polyesters are catastrophically lost during an initial degradation,[131] that is, 66% strength loss for 1.7% weight loss, the development of microbial polyesters with initial stability toward degradation is demanded for applications in disposable items such as packing materials and mulching films in agriculture. As a result of the intensive studies of hydrolyses of the polyesters by enzyme and alkali,[132,133] it has become evident that the rate of initiating degradation is dominated by the physical accessibility of the polymer structure to the abiotic attack. Thus, the crystallinity of the polyesters strongly influences the rate of hydrolysis due to low permeability of crystalline regions to degradation medium. Hydrolysis is initially restricted to the amorphous phase and to the fringes of the crystallites. Because the amorphous chains tie the crystallites together, initial hydrolysis leads to catastrophic mechanical failure even before weight loss.[131] To design the commercial degradable materials, therefore, it is necessary to control the rate of initial degradation.[134]

A desired polymer property often cannot be obtained from the material itself but through chemical or physical modification. Blending of two or more polymers is an attractive approach because of the low cost and simplicity. Blending biodegradable polymers also offers the potential in the design of biodegradable devices with controllable hydrolytic kinetics by simply varying blend composition.

The surface composition of multicomponent polymeric systems such as polymer blends is much different from the composition in the bulk depending on the surface free energy of polymer components as well as the intermolecular interaction between component polymers.[135] In general, a component of lower surface free energy is enriched at the surface in comparison to its blend partner with higher surface free energy. Because the degradation of microbial polyesters such as polyhydroxyalkanoates (PHAs) proceeds via surface erosion process and occurs first in amorphous regions, PHA-based blends can offer freedom in designing biodegradable devices with desired hydrolytic kinetics by controlling surface organization. It is obvious that degradability must be controlled so that materials maintain their mechanical integrity during use, avoiding the rapid decrease of the mechanical properties of microbial PHAs upon initial degradation.

4.1.1. Control of Enzymatic Biodegradation of Microbial Polyesters by Blending

Control of the enzymatic biodegradability of microbial polyesters is reviewed by Ha et al.[136] The enzymatic degradation can be controlled by blending microbial polyesters such as P(3HB) or P(3HB-co-3HV) with small amounts of a nondegradable polymer, such as polystyrene (PS) or poly(methyl methacrylate) (PMMA) by a solution-casting technique. Because the enzymatic degradation of P(3HB-co-3HV) initially occurs by a surface erosion process, these degradation behaviors can be explained by the surface structure of blend films when they are measured by XPS. The surface of P(3HB-co-3HV)/PS blend films reveals an excess of PS, whereas the surface of P(3HB-co-3HV)/PMMA blend films is nearly covered by P(3HB-co-3HV). The PS, which exists within P(3HB-co-3HV) spherulites at the surface, acts as a retardant toward enzymatic attack at the surface of the blend film.

The surface-enriched hydrophobic polystyrene retards the biodegradation of the less hydrophobic copolyester film at the initial stage of enzymatic attack, whereas the effect is not so prominent when PMMA is added to the copolyester due to their similar surface free energies. Ha et al. emphasized the importance of surface chemistry in controlling the enzymatic degradation of P(3HB-co-3HV) and its blend films.[137,138]

4.1.2. Control of Enzymatic Biodegradation of Microbial Polyesters by Plasma Modification

Plasma discharge processes provide powerful methods for altering the surface properties of materials without changing their bulk properties. A review has been devoted exclusively to the introduction of functional groups onto a material's surface for the improvement of adhesion, protein adsorption, and protective coatings.[139] Change in the wettability of material surface exposed to plasmas is attractive because of its simplicity. Fluorocarbon plasmas generate a fluorinated layer at the surface of nonpolar polymers such as polyethylene and polypropylene, causing the decrease in the surface wettability.[139] This fluorination shows poor adhesion between materials, but there is strong demand to modify polymer surfaces to make them more hydrophobic and less adhesive. Thus, plasma fluorination and oxidation are potentially attractive means for modifying surface wettability. This will lead to a change of the hydrolysis rate of polyesters.

To investigate the effect of surface modification on the control of the enzymatic degradation of microbial polyesters, Lee et al. carried out an experimental work using an extracellular PHB depolymerase from *Alcaligenes faecalis T1* for the P(3HB) and P(3HB-co-3HV) films before and after CF_3H- and O_2-plasma treatments.[140] The degradation of solution-cast films of P(3HB) and P(3HB-co-3HV) was carried out for a given time between 1 and 22 h at 37 °C in a 50 mM Tris-HCl buffer solution (pH 7.4) of an extracellular

Table 11. Atomic Concentrations of Plasma-Treated P(3HB), P(3HB-*co*-5% 3HV) and P(3HB-*co*-12% 3HV) Films (Error ± 5%) (Adapted with Permission from Ref 140; Copyright 2003 Wiley-VCH Verlag GmbH & Co.)

film	treatment time (s)	CF$_3$H plasma			O$_2$ plasma	
		C	O	F	C	O
P(3HB)	0	70.3	29.7	-	70.3	29.7
	10	51.6	5.0	43.4	68.0	31.6
	20	47.5	3.0	49.5	66.1	33.4
	40	47.6	2.5	49.9	67.0	32.8
	60	48.1	2.1	49.8	66.2	33.1
P(3HB-*co*-5% 3HV)	0	72.7	27.3		72.7	27.3
	10	48.9	4.8	46.4	68.3	31.1
	20	47.5	2.6	49.9	68.1	31.5
	40	47.7	3.0	49.3	67.9	31.9
	60	47.7	2.0	50.3	66.4	33.2
P(3HB-*co*-12% 3HV)	0	75.1	24.9		75.1	24.9
	10	50.9	6.4	42.7	70.3	29.5
	20	50.0	4.4	45.6	70.4	29.5
	40	49.5	3.2	47.3	70.1	29.4
	60	49.0	2.5	48.4	69.8	29.2

PHB depolymerase from *A. faecalis T1* before and after CF$_3$H- and O$_2$-plasma treatments.

Table 11 shows atomic concentration ratios of P(3HB), P(3HB-*co*-5%3HV), and P(3HB-*co*-12%3HV) films for different plasma treatments as a function of the plasma exposure time. The CF$_3$H plasma treatment quickly increases fluorine content to almost 50% of atomic percentage while it sharply decreases oxygen content in the film surface. This result suggests that the surface exposed by the CF$_3$H plasma is mainly composed of carbon and fluorine. However, the oxygen content after O$_2$-plasma treatment was just slightly increased.

It is noteworthy that after the CF$_3$H-plasma exposure, the atomic concentration of oxygen at surface of the P(3HB) film is very low, below 5%. Thus, this indicates that the components of the C$_{1s}$ are mainly composed of CH$_x$F$_y$ species, CF, C−CF$_n$, and CF−CF$_n$. This surface fluorination will lead to surface hydrophobicity and inactivity to PHB depolymerase. O$_2$-plasma-treated P(3HB) film was more oxidized than pure P(3HB) because the ratio of (C−O)/(C−C) [or (CO−O)/(C−C)] was increased by up to 15%. The results obtained by XPS experiments showed a similar tendency in the high-resolution C$_{1s}$ spectra.

Because a plasma treatment with a short time changes the topmost surface layer of a material, the surface layer modified by O$_2$ plasma cannot affect the degradation rate if it is more hydrolyzable. On the contrary, the fluorinated layer induced by plasma treatment retards degradation. The degradation rate of microbial polyesters was strongly affected by the surface wettability induced by plasma treatment because surface hydrophobicity causes the inactivity of enzyme. However, the surface hydrophilicity induced by a plasma oxidation did not show an effect on the enzymatic degradation.[140]

4.2. Hydrolysis of Degradable Poly(α-hydoxy acid)s by Surface Chemistry As a Model of Drug Delivery Systems

4.2.1. General Overview

Although the surface analytical techniques discussed in this review have proven to be powerful tools

for studying the surfaces of polymeric biomaterials,[38] only in very few instances have these techniques been used to study the kinetics of surface degradation.[126] It has been known for some time that SSIMS is more sensitive to some types of surface degradation on polymers, because of the specificity of the information and the low detection limits.

Gardella et al. studied the hydrolysis of poly(*tert*-butylmethacrylate) (PtBMA).[141] SSIMS was used in the work to analyze a system that could not be followed by routine XPS analyses. The results obtained demonstrated the capabilities of SIMS to detect the extent of a mild reaction on the surface of polymers. The work suggested SIMS has the most promising surface technique for the analysis of degradation in polymer surfaces.

The compelling need to develop biodegradable polymers for drug delivery and tissue engineering has prompted the development of analytical approaches with emphasis on both surface and bulk characterization.[1] Defining the role of surface versus bulk erosion processes is important, as mentioned in the Introduction, because the surface is the direct contact region that is expected to dictate at least the initial in vivo performance; furthermore, the surface properties cannot be always predicted from observation of the bulk properties. This is often due to a specific molecular or oligomeric orientation or composition at the surface or surface-specific chemical reactions.

In this regard, Gardella and co-workers reviewed several aspects of current work published on poly-(α-hydroxy acid)s and their associated copolymers:[141,142] They reported on the development of a new method for the quantification of the hydrolytic surface degradation kinetics of biodegradable poly(α-hydroxy acid)s using TOF-SIMS.[142] They reported results from SSIMS spectra of a series of poly(α-hydroxy acid)s including PGA, PLLA, and PLGA hydrolyzed in various buffer systems. The distribution of the most intense peak intensities of ions generated in the high mass range of the spectrum reflects the intact degradation products (oligomeric hydrolysis products) of each biodegradable polymer. First, a detailed analysis of the oligomeric ions is given on the basis of rearrangement of the intact hydrolysis products. The pattern of ions can distinguish both degradation-generated intact oligomers and their fragment ion peaks with a variety of combinations of each repeat unit. Then, the integration and summation of the area of all ion peaks with the same number of repeat units was proposed as a measurement that provides a more accurate molecular weight average than the typically used method, which counts only the most intense peak. The multiple ion summation method described in this paper would be practical in the improvement of quantitative TOF-SIMS studies as a better data reduction method, especially in the surface degradation kinetics of biodegradable polymers.[142]

The polyesters are a family of degradable polymers that has received considerable attention. As a class of polymers and copolymers, biodegradable polyesters, based on simple biological acid compounds, such as glycolic or lactic acid, are used, temporarily, as
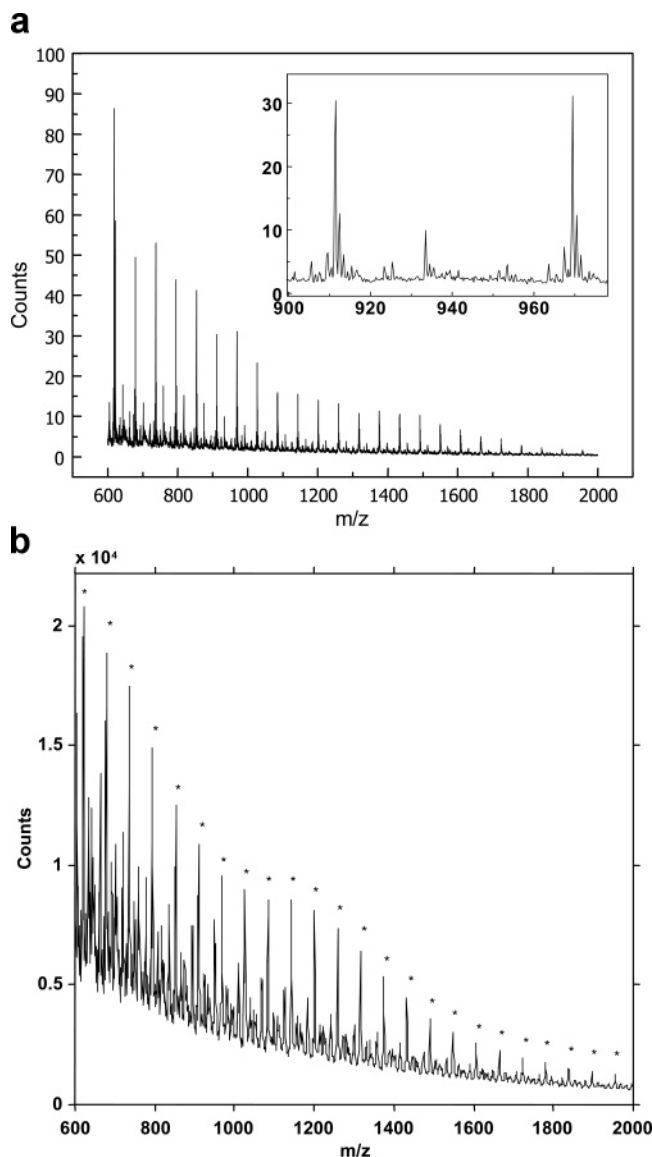
a

b

Figure 7. (a) High-mass portion of TOF-SIMS spectra of PGA hydrolyzed for 1 h. (b) High-mass portion of TOF-SIMS spectra of PGA hydrolyzed for 4 h. The maximum in molecular peak distribution is shown. (Reprinted with permission from ref 147a. Copyright 1999 American Chemical Society.)

sutures, tissue scaffolding, wound healing, and drug delivery matrices.[143–146] These polymers degrade via hydrolysis process, already mentioned in section 3. XPS is usually not capable of detecting any changes during the hydrolysis of most biodegradable polymers, including PGA, PCL, and PLA. SSIMS results demonstrated clearly the detection of the degradation of the polyesters.[147]

Figure 7a shows the high-mass portion (600–2000 Da) of TOF-SIMS spectra of PGA hydrolyzed for 1 h.[147a] Before the hydrolysis treatment, essentially no signals can be observed in this range, except simply a background. Upon hydrolysis, a peak pattern characterized by the differences due to the mass of the repeat unit of PGA was observed. All of the ions of the major peaks in Figure 7a have the structure of $[nG + H_2O + Na]^+$, where G stands for the repeat unit of PGA. The result in Figure 7a indicates that the ions detected from the hydrolyzed PGA sample

are the intact oligomers of the hydrolytic degradation products. In addition to the wide distribution of molecular ion peaks, a maximum in the molecular ion peak distribution can also be seen from 1000 to 1500 Da in the TOF-SIMS spectrum of PGA hydrolyzed for 4 h (Figure 7b). These maxima can be followed from the 1 h hydrolysis sample spectra (Figure 7a) at 1400–1500 Da and shift to lower mass ranges gradually as the hydrolysis time increases. Considering that the maxima represent the distribution of molecular weights of hydrolysis products at the particular reaction time, the TOF-SIMS data surely show us it can be utilized for the investigation of the hydrolytic degradation kinetics.

Now, let us discuss details of the hydrolysis process of each poly(α-hydroxy acid) in terms of surface chemistry.

4.2.2. Poly(glycolic acid)

PGA[148–153] is a highly crystalline, hydrophilic, linear aliphatic polyester that is the simplest biodegradable poly(α-hydroxy acid) and has been shown to undergo hydrolytic degradation both in vitro and in vivo.[154–156] It has a high melting point and a very low solubility in most common organic solvents with the exception being hexafluoro-2-propanol. Because of their biocompatibility and biodegradability, PGA and its copolymers have been studied for potential dental,[157,158] drug delivery,[159–161] and orthopedic[162] applications since their first commercial application as absorbable sutures under the trade name Dexon by the American Cyanamid Corp. in the 1970s.[163–165] Although PGA and its copolymers have been of research interest for decades, most of the work has been bulk phase studies. These have involved the use of techniques that analyze the bulk properties[166–169] such as time for total degradation, drug release profiles, extent of water absorption, total weight loss, crystallinity, tensile strength, thermal properties, and molecular weight as a function of treatment time.[154,170–173]

Chen et al. presented a new approach for studying the hydrolytic degradation kinetics of biodegradable polymers using TOF-SIMS.[174] In this study, in vitro hydrolytic degradation of PGA has been carried out at 37 °C in aqueous saline buffer solutions of different pH values. To adjust the pH of the solution, the following were used: neutral buffer condition (Isoton II, pH 7.4), sodium hydroxide adjusted Isoton II solution (pH 10.0), potassium carbonate–potassium borate–potassium hydroxide buffer solution (pH 4.0). The molecular weight distribution of hydrolysis products was obtained from the TOF-SIMS spectra. The average molecular weight of the hydrolysis products calculated from the TOF-SIMS spectra is a function of hydrolysis time as shown in Figure 8.

A multiple molecular weight distribution can be seen growing, and the second crest of the distribution (marked with arrows in Figure 8) moves toward lower molecular weight as the hydrolysis time increases.

On the basis of such TOF-SIMS results, the following kinetic equation was established:

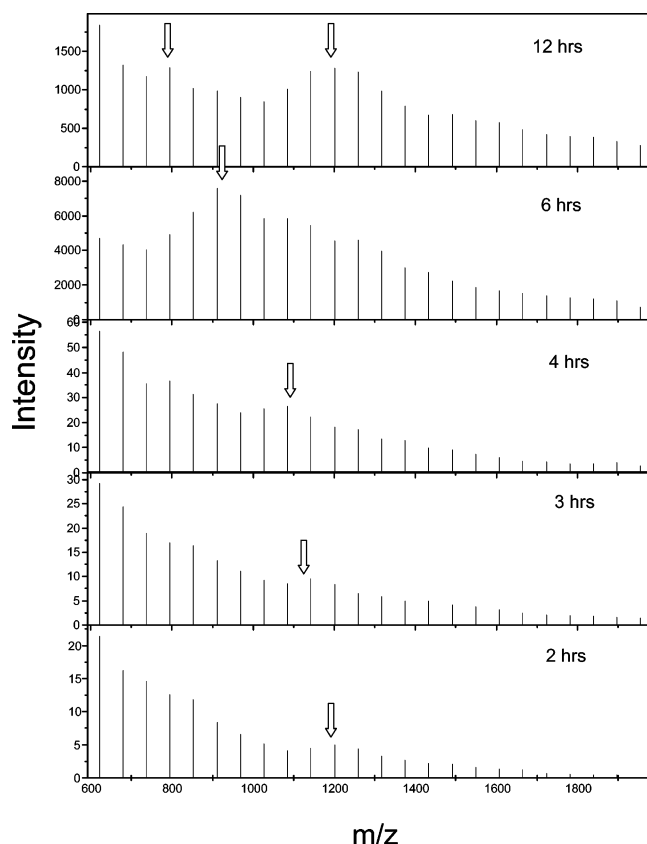$$\ln (D_t - 1)/D_t = \ln(D_0 - 1)/D_0 - k't = c - k't \quad (1)$$

Figure 8. Plots of molecular weight distribution of different hydrolysis time, calculated from TOF-SIMS spectra of PGA samples hydrolyzed in neutral saline solution. (Reprinted with permission from ref 174. Copyright 2000 American Chemical Society.)
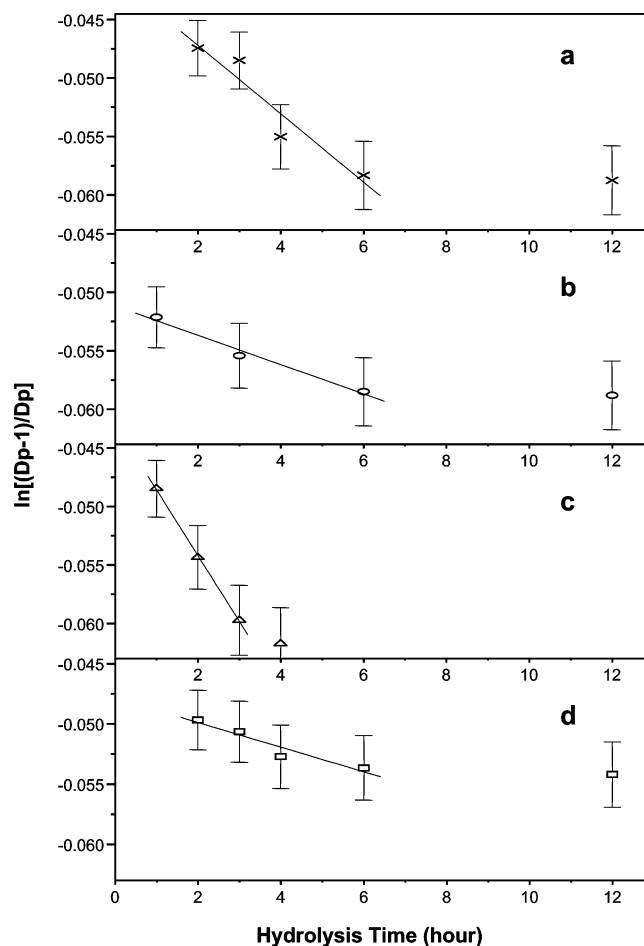

Figure 9. Semilog plot of degree of polymerization versus hydrolysis time using eq 1: (a) PGA disk sample hydrolyzed in Isoton II physiological buffer solution (pH 7.4), (b) hydrolyzed potassium hydrogen phthalate buffer solution (pH 4.0), (c) hydrolyzed in sodium hydroxide adjusted Isoton II solution (pH 10.0), and (d) hydrolyzed in potassium carbonate−potassium borate−potassium hydroxide buffer solution (pH 10.0) (Reprinted with permission from ref 174. Copyright 2000 American Chemical Society.)

c is a constant, and D_t is the average degree of polymerization at the sample surface at time t of hydrolysis. The starting molecular weight determines the intercept of the straight line if the plot of $\ln(D_t - 1)/D_t$ versus reaction time t gives a straight line.

Figure 9 shows a typical plot using eq 1. The kinetic constants calculated by regression using the first few data points in the linear relationship are summarized in Table 12. In Table 12, k' is the apparent reaction constant and k is the absolute reaction constant at the specified solution acidity.

A relative standard deviation of 5% was estimated for the reaction constants using error propagation theory, indicating good reproducibility of data for the method. A good linear relationship was obtained using this kinetics equation. The reaction rates observed in this study generally agree with observations reported in the literature. This new approach demonstrates that TOF-SIMS can be a powerful and fast technique in the study of degradation kinetics of biodegradable polymers. Using TOF-SIMS, the hydrolysis kinetics of biodegradable polymers could be explored in the range of hours with in vitro methods.[174]

Lee and Gardella studied the in vitro hydrolytic degradation of thin (~100 μm) films of PGA, focusing on the kinetics of degradation of the near surface phases.[29] In their initial study, Gardella and Hernandez de Gatica were able to demonstrate that oligomeric species were present on the surface of

Table 12. PGA Hydrolysis Reaction Constants[a] (Adapted with Permission from Ref 174; Copyright 2000 American Chemical Society)

solution	pH	k' (s^{-1})	k (s^{-1} mol^{-1})	R^2
Isoton II	7.4	0.0029	5.2×10^{-5}	0.92
acidic buffer	4.0	0.0013	2.3×10^{-5}	0.98
Isoton II/NaOH	10.0	0.0055	9.9×10^{-5}	0.99
basic buffer	10.0	0.0013	2.3×10^{-5}	0.98

[a] Five percent relative standard deviation applies to reaction constant results.

thick (~1 mm) plates of PGA after exposure to in vitro hydrolysis conditions.[2a] In that work, however, they did not control the crystallinity of the thick samples or study the degradation rate of crystalline versus amorphous regions. In addition, it is known[174] that boric acid, a Lewis acid, generated in potassium carbonate−potassium borate−potassium hydroxide buffer (pH 10.0) during the hydrolysis treatment of PGA samples could have a retardation effect on the hydrolytic surface degradation.

It is known that a bulk erosion mechanism[154,175,176] based on both in vivo and in vitro observations is responsible for the main degradation of biodegradable
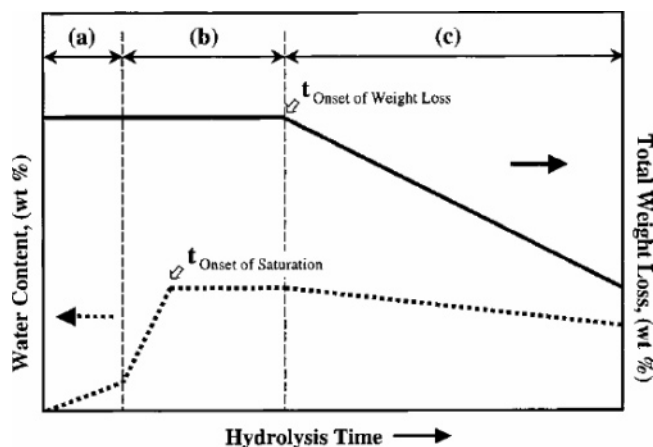
Figure 10. Descriptive hydrolytic bulk erosion profile for semicrystalline biodegradable polyesters: (a) incubation; (b) induction; (c) polymer erosion. (Reprinted with permission from ref 26. Copyright 2001 American Chemical Society.)

polyesters: random chain scission on the linkage of ester bonds in the polymer backbone proceeds homogeneously throughout the matrix. The bulk degradation pathway[154,175,176] has three major features in the polymer erosion profile (Figure 10): (1) incubation, without changes in weight and molecular weight (MW), which reflects the interval required for water penetration into the polymer matrix; (2) induction, with a decrease in MW and a rapid increase in the degree of matrix hydration followed by saturation; and (3) onset of polymer erosion (weight loss) and any changes in the rate of chain scission.[26] Recently, however, it has been reported that large devices of biodegradable polyesters degrade via a heterogeneous mechanism;[177] that is, the degradation proceeds more rapidly in the center than at the surface. This is attributed to the autocatalytic action of the carboxylic acid end groups of degradation products that are trapped in the matrix.

By fabricating a thinner sample with reproducible crystallinity and using other buffer systems without borate as a chemical component, Lee and Gardella further investigated the role of the surface-segregated amorphous fraction influencing surface and bulk degradation at different buffered pH values during the induction period of bulk erosion processes with increasing hydrolysis time. Physical, chemical, and morphological studies of the PGA films were carried out using TOF-SIMS as well as SEM and XPS for the surface determination and DSC for the bulk thermal properties and weight loss studies for the confirmation of induction period.

The initial "induction" period of hydrolysis at the surface of PGA-based devices is important in drug delivery and in the understanding of surface/interface reactions related to inflammation[178] in many in vivo applications of biodegradable polyesters. In vitro studies of the hydrolytic degradation of PGA reported in this work present the role of surface amorphous region at the initial stage of erosion profile on surface versus bulk degradation processes in three different pH buffer media. A combination of SEM, XPS, and TOF-SIMS provides surface characterization, and DSC and weight loss studies provide results from the

Table 13. Molecular Weight Characterization Results for PGA Hydrolysis Products at the Surface (Adapted from Reference 26)

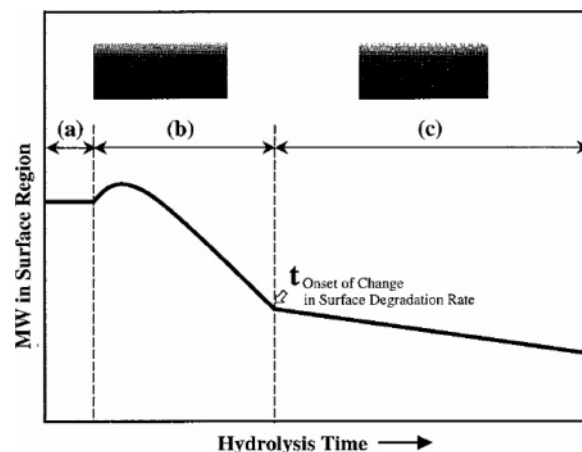| time (h)	Isoton II (pH 7.4)		carbonate buffer (pH 10.0)		biphthalate buffer (pH 4.0)	
	M_n	PI	M_n	PI	M_n	PI
1	879.2	1.11	940.0	1.14	872.8	1.11
2	931.3	1.14	958.5	1.14	895.4	1.12
3	958.4	1.16	947.6	1.13	898.4	1.12
4	954.3	1.16	936.3	1.14	887.7	1.10
6	947.0	1.14	920.0	1.12	867.6	1.11

Figure 11. Descriptive MW profile in the surface region of thin (100 μm) PGA films: (a) incubation; (b) onset of abrupt MW change; (c) decrease in surface degradation rate. (Reprinted with permission from ref 26. Copyright 2001 American Chemical Society.)

bulk phases of the film. During the first 6 h of exposure no change in weight loss is detectable, yet morphological changes occur at the surface of PGA as observed by SEM. In particular, TOF-SIMS shows the formation of oligomeric hydrolysis products presumably adsorbed at the surface; these data have been quantified to extract the MW of the hydrolysis products and to finally establish the hydrolytic surface degradation kinetics in various pH buffers.

The intensities of the four peaks with the same repeat number (n) on the TOF-SIMS spectra were integrated together to represent the total intensity (N_i, $i = n$) for the particular PGA oligomer ($M_i = nM_{mom} + H_2O$) over the range from 600 Da to the last detectable peak, where $M_{mom} = 58.01$ amu, the repeat unit of PGA. The database was subsequently analyzed using the conventional statistical averaging definitions for the number-average molecular weight and weight-average molecular weights and the polydispersity index (PI). The results are summarized in Table 13. The decrease in M_n of intact hydrolysis products produced at the surface was observed from 2 or 3 h of hydrolysis time after the initial increase. The initial increase of MW followed by a decrease during the induction period is attributed to the preferential degradation of the surface-segregated amorphous fraction. As a result, they suggested a descriptive MW profile in the surface region of thin (100 μm) PGA films including very short incubation (a), onset of abrupt MW change (b), and decrease in surface degradation rate, as shown in Figure 11.

The effect of surface degradation on the bulk thermal properties was investigated by comparing TOF-SIMS data to the corresponding crystallinity change in the bulk. XPS data showed the addition of small amounts of sodium at the surface but no sensitivity to the changes in surface chemistry. The hydrolytic degradation rates at the surface of PGA are 3 times faster in both pH 4.0 sodium biphthalate and pH 10 sodium carbonate buffers than in pH 7.4 physiological electrolyte buffer (Isoton II).

These results allow three important conclusions about the surface reactivity of PGA-based devices. The surface region is enriched in amorphous PGA more than the interior of the device; thus, the rapid reaction kinetics associated with amorphous polymers dominates the initial reaction period. During the induction period, when few changes in overall device mass may occur, rapid reactions over the top few nanometers predominantly generate short-chain polymeric oligomers with very little solubility to the surrounding aqueous phase.

Yet, this reactivity could affect a significant initial burst of additives such as drugs being delivered and presumably induce a local decrease in pH. The lower local pH could significantly increase the reaction rate of the surface as acid and base conditions away from physiological pH increase reaction rates. Therefore, the chemistry of the induction period is dominated by surface and interfacial reactions until the equilibration of water penetration and absorption leads to bulk degradation processes. Both surface and bulk characteristics could be examined over the hydrolysis time beyond an induction period to define the change in hydrolytic surface degradation kinetics due to the onset of weight loss and also the release profile of the soluble fraction using liquid chromatography (LC)−mass spectrometry (MS).

4.2.3. Poly(DL-lactic acid)

PLA is another important biodegradable aliphatic polyester approved by the U.S. FDA for human clinical use including in tissue engineering as scaffolds to direct specific cell growth and differentiation as well as drug carriers. Thus, PLA has been one of most widely used biodegradable polymers for drug delivery systems and porous scaffolds.[178,180]

Davies and co-workers determined the erosion behavior of blends of PLA and the more reactive poly(sebacic anhydride) (PSA) by the chemical composition and the molecular organization of the surface of the materials.[24] In their study they have characterized the surfaces of immiscible and miscible blends of the PSA and PLA using the surface techniques of SSIMS, XPS, and AFM. SSIMS and XPS have recorded the surface enrichment of all of the blends with the PLA component. For the immiscible blends, differential charging within the XPS spectra also provided evidence of phase separation. AFM data have contrasted the surface morphologies of the immiscible and miscible blends, and the use of in situ AFM techniques has enabled the effect of blend morphology on surface erosion to be visualized. For the immiscible systems, clear phase separation morphologies can be observed, and at certain blend

compositions the rapid loss of the PSA from the films results in the exposure of the PLA morphology. However, as the PLA content is increased, the surface enrichment effect results in the degradation behavior of the blend being dominated by the slow-degrading PLA surface layer. For the miscible systems, the in situ AFM studies visualized a disintegration of the whole blend film without the exposure of a PLA morphology, indicating that the hydrolysis of the PSA component rendered the whole film unstable. The use of SIMS, XPS, and AFM, while highlighting the complexity of polymer blend surfaces, could provide a rapid analysis of the physicochemical phenomena underlying the organization of these systems and therefore should facilitate the application of such systems as biomaterials.[24]

4.2.4. Poly(DL-lactide-co-glycolide) (PLGA)

PLGA is another classic biodegradable polymer that has been well studied and documented because of its excellent tissue compatibility, biodegradable nature, and safety profile for use in humans.[181] Considerable burst release of drugs from PLGA nanospheres and microspheres was frequently observed due to high drug loading, small particle size, and short diffusion path for surface-associated drug molecules[179] as already shown in section 3. The degradation rate of PLGA is dependent upon its composition and molecular weight. Both lactic and glycolic acids are produced within the degrading PLGA matrix, resulting in an acidic microenvironment that contributes to the bulk erosion of the matrix.[183,184]

A thorough understanding of the factors affecting the drug release mechanism from surface-erodible polymer devices is critical to the design of optimal delivery systems. Drug release rates can be controlled by manipulation of the particle size, the polymer degradation and/or erosion rates, and the polymer erosion mechasinm (bulk versus surface erosion) among other factors. For example, surface-eroding polymers such as polyanhydrides may simplify the drug release kinetics because the drug release rate becomes dependent predominantly on the polymer erosion rate. However, drug release and polymer erosion rates are sometimes not correlated, depending on the copolymer composition or the relative hydrophobicity of the comonomers for the copolymer case and the miscibility of the drug with the polymer.[181a] Some examples of PLGA loaded with drug for drug delivery system were discussed in section 3.

There are contradictory results about the influence of the pH of the external medium on the rate of bulk degradation. Acceleration of the degradation rates at low[171] pH as well as high[172,173] pH values has been reported, yet other results[154,170] showed pH-independent hydrolysis in vitro. Reed and Gilding[170] reported that the insensitivity of pH on hydrolytic degradation kinetics was due to the combined effects of hydrophobic/hydrophilic balance and crystallinity in the experiments performed with PLGA as well as PGA. The extent of water hydration was thought to determine the rate of degradation; this is supported by the

fact that amorphous PLGA[171] was degraded more quickly than semicrystalline PGA, and a lower rate of degradation was observed for stereoregular PLLA relative to amorphous PDLLA.[175]

Following an accelerated degradation testing of these polymers, however, Dauner et al.[185] showed that no significant effect from the crystallinity was detected. Li et al.[186] reported that degradation-induced morphology changes of large-size amorphous PDLLA devices were observed during degradation with the partial crystallization of degradation byproducts or residues. Hence, the degradation of PLGA as well as PGA and PLA may be significantly influenced by many factors such as the morphology and crystallinity of the material and formulation, besides the structure, molecular weight, and composition of the polymers. The amorphous fraction, which is assumed to be surface segregated from AFM studies[24,187] on a series of biodegradable polymers, may also play a role in both bulk and surface degradation in order to explain the roles of morphology and crystallinity on surface and bulk reaction kinetics.

4.2.5. Hydrolytic Degradation of Polyester Monolayers at the Air/Water Interface

Many different analytical methods have been applied to determine the degradation rate of polyesters. One suitable technique to study the hydrolysis behavior is to use a Langmuir film balance to study polymers at the air/water interface, because the hydrolysis of a polyester usually occurs through the cleavage of ester groups and eventually produces water-soluble oligomers and monomers.

The hydrolysis of polyester monolayers would result in a change in the occupied area when the monolayer is maintained at a constant surface pressure. The study of polyester monolayers at the air/water interface will, therefore, give a fundamental understanding of the hydrolytic mechanism of polyesters, such as polymers and copolymers derived from lactic acid (LA), glycolic acid (GA), and ϵ-caprolactone (CL). There have been several reports on the structural study of polyester monolayers at the air/water interface.[188,189] Ivanova et al. reported the hydrolytic behavior of poly(DL-lactide) monolayers spread on acidic (pH 1.9 by HCl) and basic (pH 11.4 by Na_2HPO_4 and NaOH) subphases for short times.[190] They calculated the hydrolysis rates by assuming that the reaction products from fragment hydrolysis are soluble when the number of lactic units in sequence is below 4.[191]

Lee and Gardella studied[192] systematically the hydrolytic degradation of PDLA and PLLA, PCL, poly(l-LA-co-CL), and a blend (1:1 by mole) at the air/water interface as a function of degradation medium, pH, and time. The hydrolysis of polyester monolayers strongly depended on both the degradation medium used to control subphase pH and the concentration of active ions. Under the conditions studied, polymer monolayers showed faster hydrolysis when they were exposed to a basic subphase rather than that of acidic or neutral subphase. The basic (pH =10) hydrolysis of PLLA/PCL (1/1 by mole) blend was faster than that of each homopolymer at the initial stage. This result is explained by increasing numbers of base attack sites per unit area owing to the very slow hydrolysis

of PCL, a "dilution effect" on the concentration of PLLA monolayers. Conversely the hydrolytic behavior of poly(l-LA-co-CL) (1/1 by mole) was similar to that of PCL even though the chemical compositions of the blend and the copolymer are very similar to each other. The resistance of the copolymer to hydrolysis might be attributed to the hydrophobicity and the steric hindrance of the CL unit in the copolymer. The model system served to describe the role of the initial steps in degradation, those occurring through the interfacial or surface limited cleavage of ester groups, which eventually produces water-soluble oligomers and monomers.[193]

On the other hand, parameters affecting the controlled degradation of blends include composition,[194,195] preparation method,[194] miscibility,[10b,195] and degree of surface segregation of one component with lower surface energy.[24] Biodegradable polymer blends, some of which create heterogeneous microstructures due to physical mixing, will show different hydrolytic behaviors for each blend component. It is important to know the degradation rate of each component in a blend system and how this rate can be affected by morphology.

One possible application of such a differentially biodegradable blend is for drug release using the resulting different degradation rates of each component. Two kinds of drugs, which have different medical efficacies, could be delivered at the same time with different controlled release times if they can be partitioned into the different phases. However, little is known about the hydrolyzability of each individual component in a polymer blend.

Lee et al. further reported on the magnitude of the dilution effect and the acceleration of the hydrolytic rate of biodegradable polymer blend monolayers, using the Langmuir monolayer technique.[193] The hydrolytic behavior of monolayers of biodegradable PLLA/PCL blends spread at the air/water interface was studied to identify the relative rate of hydrolytic degradation of each component when exposed to a basic subphase. As the hydrolysis time increases, the isotherm recorded from PLLA/PCL blend monolayers was found to be similar to that of PCL homopolymer; this is likely to be due to the preferred hydrolysis of PLLA. The rate of hydrolysis was recorded by a change of occupied area when the monolayer is maintained at a constant surface pressure. The hydrolysis of the blend in a basic condition was much faster than that of each homopolymer, regardless of the composition, arising from a dilution effect on the concentration of PLLA monolayers. From the deviation behavior ($D_{t,blend}$) in the area ratio of each blend between the arithmetic average ($X_{t,blend}$) and experimental values ($x_{t,blend}$), blends with compositions of <50 mol % PLLA showed the maximum dilution effect, whereas high PLLA compositions (>75 mol % PLLA) showed a smaller effect, as shown in Figure 12. In this figure, the curves were calculated by using eq 2.

$$D_{t,blend} = 1 - x_{t,blend}/X_{t,blend} \qquad (2)$$

The excess of blend hydrolysis due to the dilution effect can be expressed by the sum of the deviation (ΣD_t). The negative slope in the nonlinear region was
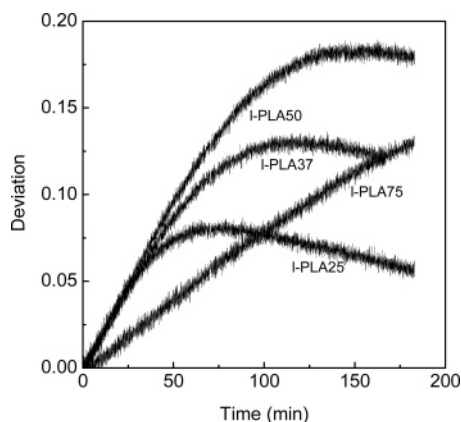
Figure 12. Deviation versus time for (PLLA/PCL) blend monolayer films maintained at 7 mN/m on the subphase of pH 10.5. The curves were calculated by using eq 2. l-LA is the same as PLLA. (Reprinted with permission from ref 193. Copyright 2002 American Chemical Society.)

explained in terms of the hydrolysis of the remaining PCL and the residual effect of preferentially hydrolyzed PLLA.

4.2.6. Poly(β-malic acid)

The surface chemical structure of poly(β-malic acid), especially poly(ortho esters), and its ester derivatives was analyzed by Davies and co-workers using TOF-SIMS and XPS.[181b]

Poly(ortho esters) (POEs) are a versatile family of biodegradable and biocompatible polymers and are receiving significant attention because they can be designed to possess a surface-dominant erosion mechanism and, thus, provide a zero-order release profile for various therapeutic agents.[184,196]

The pH sensitivity of the POEs has led to several drug delivery systems being developed, of which the rate of drug release is predominantly controlled by the rate of polymer hydrolysis. Davies's group used XPS, SIMS, and AFM in a multitechnique approach to probe the effect of acid-catalyzed hydrolysis at the interface of POEs. They analyzed positive ion SIMS spectra in the range m/z 100−300 before and after hydrolyzing the POE 3,9-diethylidene-2,4,8,10-tetraoxaspiro[5,5]undecane-*co*-N-phenyldiethanolamine (DETOSU/PDE) in 0.001 M HCl for a given time. Figure 13 shows their typical positive ion SIMS spectral result. From the relationship between the relative intensity of the m/z 231 cation of $[M_{DETOSU} + H]^+$ (where M is the mass of the monomer unit) and the time of exposure in the acid solution, they suggested that the preferred mechanism for hydrolysis was via the cleavage of an exocyclic alkoxy bond in the 3,9-diethylidene-2,4,8,10-tetraoxaspiro[5,5]-undecane (DETOSU) unit (Scheme 2). The cation has the structure below:
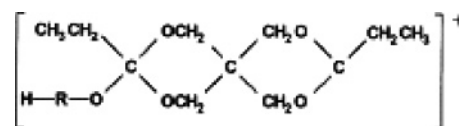
The molecular specificity of SIMS was successfully employed in their work, whereas the resulting change in the surface chemical structure of the partially hydrolyzed POE is such that it was not detectable by XPS analysis. Images acquired from an in situ AFM study of the hydrolysis of a POE showed changes in the surface morphology, seen as the formation of pits, and an overall thinning of the
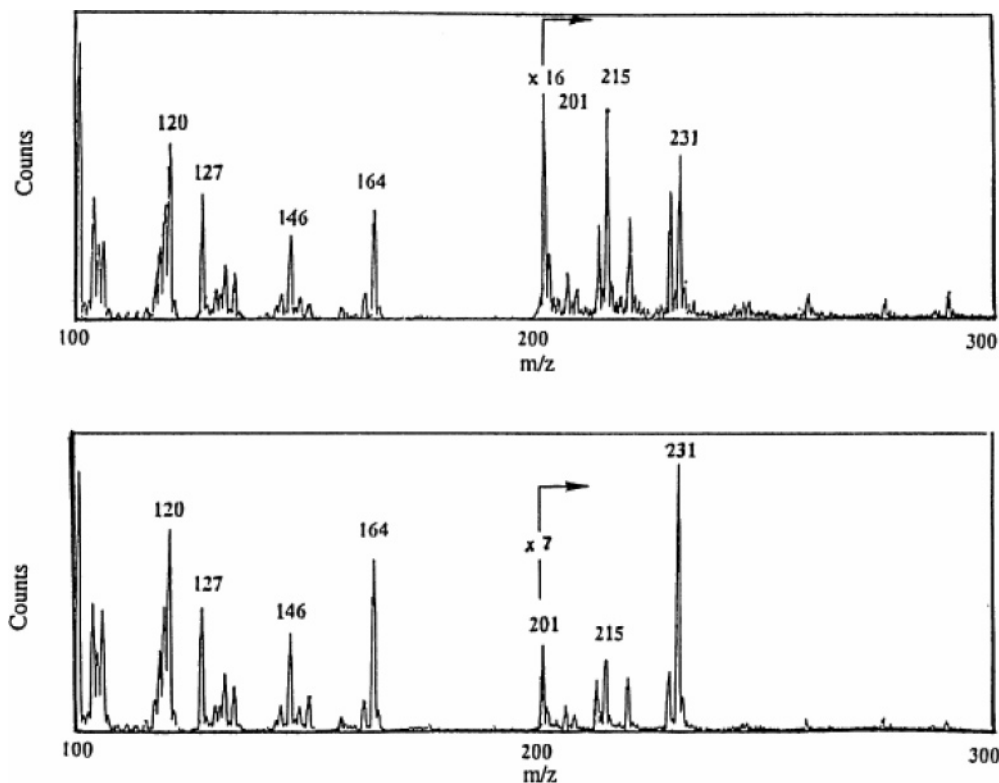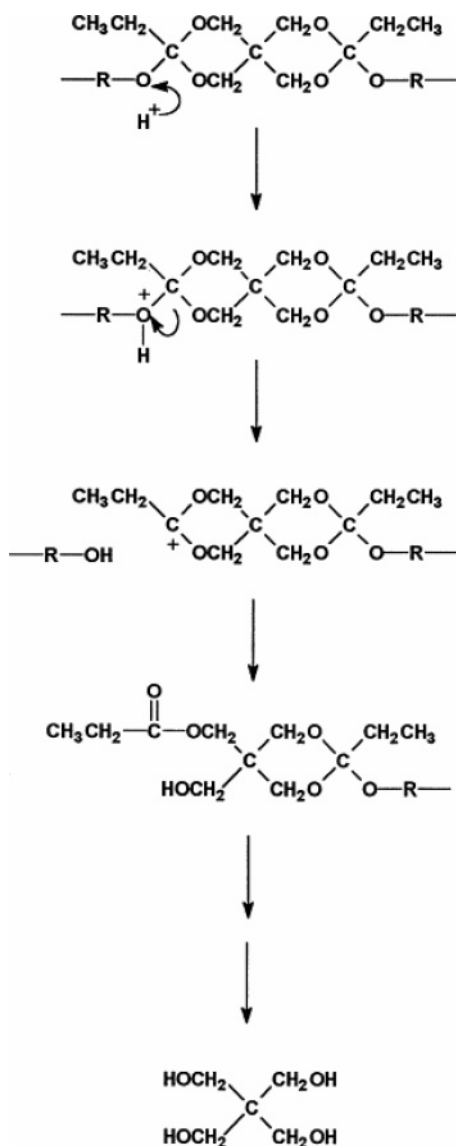

Figure 13. Comparison of the positive ion SIMS spectra of (a) DETOSU/PDE and (b) a film of DETOSU/PDE exposed to 0.001 M HCl for 2.5 min. (Reprinted with permission from ref 181b. Copyright 1998 Elsevier Science Ltd.)

Scheme 2. Proposed Mechanism for Exocyclic Alkoxy Bond Cleavage in DETOSU (Reprinted with Permission from Reference 181b; Copyright 1998 Elsevier Science Ltd.)

polymer film. The use of SIMS, XPS, and AFM has enabled changes in surface chemistry to be compared with changes in surface morphology. These complementary data, on the behavior of the polymer during degradation, have important implications for the further design of novel biodegradable materials.[181b,184]

Wang et al. fabricated the physostigmine-loaded POE, PLGA, and POE/PLGA blend microspheres by a spray-drying technique, for which the structure of the physostigmine is as follows:[184]

Physostigmine: $C_{15}H_{21}N_3O_2$
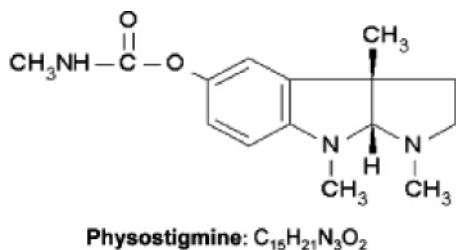
The in vitro degradation of, and physostigmine release from, the microspheres were investigated.

SEM analysis showed that the POE and POE/PLGA blend particles were spherical. They were better dispersed when compared to the pure PLGA microspheres. Two glass transition temperature (T_g) values of the POE/PLGA blend microspheres were observed due to the phase separation of POE and PLGA in the blend system. XPS analysis proved that POE dominated the surfaces of POE/PLGA blend microspheres, indicating that the blend microspheres were coated with POE. The encapsulation efficiencies of all the microspheres were >95%. The incorporation of physostigmine reduced the T_g value of microspheres. The T_g value of the degrading microspheres increased with the release of physostigmine. For instance, POE blank microspheres and physostigmine-loaded POE microspheres had T_g values of 67 and 48 °C, respectively. After 19 days of in vitro incubation, T_g of the degrading POE microspheres increased to 55 °C. Weight loss studies showed that the degradation of the blend microspheres was accelerated with the presence of PLGA because its degradation products catalyzed the degradation of both POE and PLGA. The release rate of physostigmine increased with the increase of PLGA content in the blend microspheres. The initial burst release of physostigmine was effectively suppressed by introducing POE to the blend microspheres. However, there was an optimized weight ratio of POE to PLGA (85:15 in weight), below which a high initial burst was induced. They suggested that the POE/PLGA blend microspheres may make a good drug delivery system in that the initial burst release of physostigmine can be suppressed with the presence of a POE coating layer in the blend microspheres by improving the hydrophobicity of the microsphere system while a sustained release of the model drug is obtained.

4.3. Initial Burst of Drug Release Coupled with Polymer Surface Degradation: PLLA Case

The drug release kinetics from drug/biodegradable polymer blend matrices are found to be complicated because of both polymer erosion and drug diffusion through preformed microporous channels within the matrices.[175,197] Factors such as the morphology and crystallinity of a polymer, formulation, drug molecular size, and water solubility may have significant influence not only on the degradation of drug delivery devices but also on the release profile of a drug. Furthermore, it has been reported in previous studies that it is difficult to predictably control drug release over a desired period.[198] This is caused by an initial burst (rapid release) of drug combined with the process of relatively faster drug diffusion than polymer degradation of the matrices. Although a number of studies[197–199] have been directed toward drug release profiles and correlating these results with polymer degradation kinetics, no attempt has been made to simultaneously determine both at the surface during the induction period of bulk erosion of drug/biodegradable polymers, especially PLLA blend matrices.

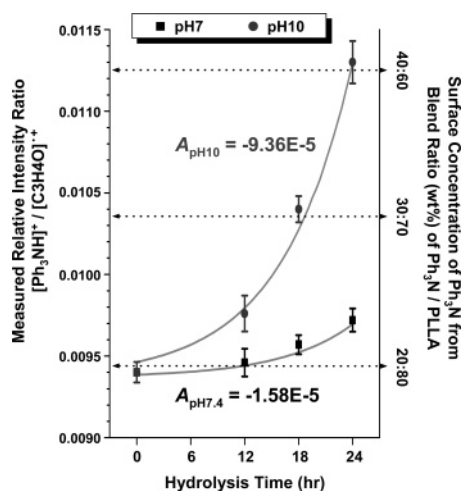As a model system of drug delivery, Lee and Gardella[200] have chosen PLLA as a matrix biode-

Figure 14. (Left Y axis) Concentration of Ph_3N accumulated at the surface of Ph_3N/PLLA (20:80 wt %) blend matrices as a function of hydrolysis time in two pH buffered conditions, respectively. The curves were fit with an empirical exponential expression, $([Ph_3NH] + /[C_3H_4O]^{•+}) = -9.37E-3 + A$ $e \wedge (t/7.94)$: $A_{pH10} = -9.36E-5$ for pH 10.0 and $A_{pH7.4} = -1.58E-5$ for pH 7.4. (Right y axis) Surface concentration of Ph_3N obtained from the standard calibration for surface concentration of Ph_3N as described in the Experimental Section of ref 200. (Reprinted with permission from ref 200. Copyright 2003 Springer).

gradable polymer system. They also have chosen triphenylamine (Ph_3N: fw 245.33, insoluble in 100 g of H_2O, pK_b not applicable[201]) as a low MW hydrophobic model drug to minimize the diffusion and/or solubility effects of a drug depending on intrinsic basicity in the course of PLLA degradation. Because the in vivo delivery of hydrophobic drugs cannot be approximated using simple release studies into aqueous buffers, they used a method to measure surface concentration as a better means to model the availability of a hydrophobic drug in vivo.

They investigated the local pH effect on the release of a model pH-inert hydrophobic drug coupled with polymer degradation at the induction phase of biodegradable polymer erosion for better understanding the nature of initial burst of a drug. Using a novel approach with TOF-SIMS,[202] both the surface concentration of Ph_3N and degradation kinetics of PLLA are simultaneously and independently determined from a model Ph_3N/PLLA (20:80 wt %) blend matrix ($t \approx 0.4$ μm on 1.0 cm^2). In vitro hydrolysis of the model blend matrix was investigated for short-term periods (<24 h) at physiologic pH and temperature and compared to basic pH. They found that the rate of PLLA degradation was accelerated by a factor of ~3 when using basic pH in vitro, but the rate of Ph_3N accumulation at the surface was accelerated by a factor of ~6 (Figure 14).

They developed a new quantitative method to examine the earliest stages of polymer degradation and drug release. It was applied to a model system that could not be examined by traditional in vitro methods. For the model system studied the release of a low molecular weight hydrophobic drug at the induction phase of polymer erosion is related to but not singularly dependent on degradation kinetics.

To determine the concentration of Ph_3N at the surface, they tested the hypothesis that hydrolysis would change intensities of ions related only to the polymer matrix. A peak at m/z 246 in the spectrum of pure PLLA is overlapped with $[Ph_3NH]^+ = 246$ Da. The relative intensities (a peak at m/z 246/$[C_3H_4O]^{•+}$) of pure PLLA matrices were measured after the hydrolysis under two different pH-buffered conditions for 24 h, respectively: 2.62E−3 for pH 7.4 and 2.59E−3 for pH 10.0. They indicated that the relative intensity of the peak at m/z 246 ratioed to the intensity of $[C_3H_4O]^{•+}$ in pure PLLA is independent of pH and hydrolysis time. Therefore, it is valid to use the change in the ratio of intensities, m/z 246 divided by m/z 56, as a measure of release profiles that represent a change in the surface concentration of Ph_3N.

The surface concentration of Ph_3N from the 20:80 wt % blend matrices has been measured as a function of hydrolysis time at two buffered pH values and compared with the corresponding concentration from a series of Ph_3N/PLLA blend matrices, as shown in Figure 14 for evaluating the cumulative amount of Ph_3N. The rate of increase in relative intensity of $[Ph_3NH]^+/[C_3H_4O]^{•+}$ at basic buffered pH ($A_{pH10} = -9.36E-5$) is 5.92 times faster than that in physiologic buffered condition ($A_{pH7.4} = -1.58E-5$). To better understand the role of the environmental pH effect on the drug release behavior coupled with polymer degradation at the surface/interface of PLLA blend matrices, the surface concentration profiles of Ph_3N have been compared with the corresponding hydrolytic degradation kinetics of PLLA in each pH condition. The extent of change in accumulation rate of Ph_3N ($A_{pH10} = -5.92A_{pH7.4}$) is >2 times greater than that in the hydrolytic degradation rate of PLLA ($k_{pH10} = -2.67k_{pH7.4}$) at the surface of Ph_3N/PLLA (20: 80 wt %) blend matrices.

They also carried out TOF analysis of drug surface concentration and polymer degradation kinetics in biodegradable PLLA blends.[203] In their paper, they reported a quantitative method of analyzing both the earliest stage of degradation of a polymer and the surface concentration of an additive using TOF-SIMS. The SSIMS spectra of Ph_3N/PLLA (20:80 wt %) blend matrices hydrolyzed in buffered conditions within a short-term (<48 h) period are simultaneously analyzed in the low-mass range for the surface accumulation profile of Ph_3N and in the high-mass range to determine the hydrolytic degradation kinetics of PLLA, respectively. The results provided new insight in evaluating the surface concentration of Ph_3N ($pK_b = 0$) from the blends to see how it relates to the reactions (hydrolytic PLLA degradation) occurring in the surface region in the initial induction period over which negligible loss of polymer weight is observed. The relative PLLA surface degradation at pH 10.0 was similar to 2 times faster than that at pH 7.4. The relative extent of increase in Ph_3N surface concentration assayed in the pH 10.0 buffer system was 9 times greater than that at pH 7.4. The initial rapid increase in surface concentration of Ph_3N was related to but not singularly

dependent on the rate of PLLA degradation at the surface of blend matrices.

They further performed simultaneous TOF-SIMS analysis to determine both the earliest stage of polymer degradation and the surface concentration of a drug additive. The static SIMS spectra of a model Ph_3N/PLLA (20:80 wt %) blend matrix ($t \sim 0.4$ μm on 1.0 cm^2) hydrolyzed in buffered conditions are simultaneously and independently analyzed in the low-mass range for the surface accumulation profile of Ph_3N and in the high mass for the hydrolytic degradation kinetics of PLLA, respectively. The rate of PLLA degradation at pH 10.0 is $\sim$2 times faster than that at pH 7.4, but the corresponding rate of Ph_3N accumulation at the surface is accelerated by a factor of $\sim$10.5.[210] The evaluation of the surface concentration of Ph_3N ($pK_b = 0$) from the blends indicates that the initial rapid increase in surface concentration of Ph_3N is related to but not singularly dependent on the rate of PLLA degradation, as for their previous work.[203]

4.4. Other SIMS Investigation on Biodegradable Polymers in Drug Delivery Systems

Cluster primary ion sources (such as SF_5^+) have generated considerable interest for organic SIMS analysis, where they have resulted in significant improvements (up to 100-fold) in characteristic molecular secondary ion yields and in some samples have resulted in decreased beam-induced damage.[205] This decreased beam-induced damage coupled with an increased sputter rate has led to the ability to depth profile some organic materials without the characteristic rapid signal decay observed with monatomic primary ion sources. More importantly, depth profiling polymer samples has been achieved for the first time with limited success.[205a]

Very recently, Mahoney et al.[206] investigated the utility of cluster SIMS in depth profiling of materials commonly utilized in drug delivery. The behavior of various biodegradable polymer films (PLA, PGA, and PCL) as well as some model drugs (theophylline, 4-acetamidophenol) under dynamic SF_5^+ primary ion bombardment is explored as a function of primary ion dose. Furthermore, a series of PLA films containing various concentrations of 4-acetamidophenol were analyzed under similar conditions. They wanted to illustrate that the distribution of a drug can be monitored as a function of depth. The resultant molecular depth profiles obtained from these polymer films doped with drug showed very little degradation in molecular signal as a function of SF_5^+ primary ion dose, and it was found that the molecular ion signals of both polymer and drug remained constant for ion doses up to $\sim$5 $\times$ 10^{15} ions/cm^2. In addition, the polymer film/silicon interface was well-defined, which may imply that sputter-induced topography formation was not a significant limitation. These results suggest that the structure of the biodegradable polymers, which all have the common main-chain structural unit of R$-$CO$-$O$-$R, allows for a greater ability to depth profile due to ease of bond cleavage. Most importantly, however, they suggested that in the particular biodegradable polymer systems, the

distribution of the drug as a function of depth can be monitored under dynamic SF_5^+ primary ion bombardment.[206]

Before conclusion are drawn, it should be noted that the kinetic approach using surface chemistry to investigate degradation behavior is not limited to drug delivery systems but can be applied to a variety of different systems for environments and biological systems. One example includes the analysis of early stages of degradation of polysulfide sealants in an aqueous environment by Church et al.[207] They used XPS and TOF-SIMS for that purpose; polysulfide sealants are widely used to ensure the integrity of fuel tanks on both civil and military aircraft, and the consequences of the failure of such sealants are severe in terms of both the length of time that the aircraft will be removed from service and the nature of the remedial work that must be carried out within the tanks themselves.

5. Conclusions

Surface science techniques can have a clear and definitive role for a biodegradable polymers, because many biodegradable materials have been designed as biomaterials for active applications. The degradation can proceed either in the bulk or at the surface of the material. A quantitative description of the role of surface degradation processes versus bulk erosion is of great importance. Although studies of the surface of biodegradable polymeric materials have provided chemical composition, structural information, or images of the morphological changes for visualization during hydrolytic or enzymatic degradation, there have been few reports of quantitative results about the surface degradation behavior. Surface studies of the reactivity of biodegradable polymers have an essential value, not only for a fundamental understanding of hydrolytic surface degradation kinetics as a model for the drug delivery systems but also toward the design and formulation of new biodegradable polymers and their fabrication into new devices. In this paper, therefore, we critically review the role of surface science in the surface reactivity to contribute to the understanding of biodegradation kinetics and controlled drug release mechanisms for some important biological polymers such as poly(glycolic acid) and poly(lactic acid).

XPS and SIMS are simple and very powerful surface analytical techniques. Especially, the development of TOF-SIMS is an area of great current interest, because TOF mass analysis gives the ability to detect ions of very high mass and therefore analyze high molecular weight samples (10000$-$20000 amu) as well as very low limits of detection due to the quasi-simultaneous detection of all masses. Previous limitations with respect to quantitation are no longer a primary barrier. Developments in quantitation methods have allowed detailed insight into reaction rates, mechanisms, and their relationship to drug release.

Clearly, there is a role for modern surface science techniques to play in understanding the mechanisms of the surface degradation reactions of biodegradable polymers.

6. Acknowledgments

The work was supported by the National Science Foundation Analytical and Surface Chemistry program, in particular, Grants CHE 0079114 and CHE 0316735 to J.A.G. C.-S.H. thanks the Research Foundation, The State University of New York, U.S.A., the National Research Laboratory Program, Korea, and the Center for Integrated Molecular Systems. (SRC/ERC Program of MOST/KOSEF (Grant Number R11-2000-070-05004-0)).

7. References

(1) Langer, R. *MRS Bull.* **1991**, Sept, 47.
(2) (a) Gardella, J. A.; Hernandez de Gatica, N. L. *J. Electron. Spectrosc. Relat. Phenom.* **1996**, *81* (3), 227. (b) Schamerger, P. C.; Gardella, J. A. *Colloid Surf. B: Biointerf.* **1994**, *2*, 209. (c) Zhuang, H.; Gardella, J. A. *MRS Bull.* **1996**, *21,* 43.
(3) (a) Kasemo, B. In *The Surface Characterizaton of Biomaterials*; Ratner, B. D., Ed.; Elsevier Science Publishers: Amsterdam, The Netherlands, 1988. (b) Kasemo, B. *Curr. Opin. Solid State Mater. Sci.* **1998***, 3* (5), 451. (c) Kasemo, B. *Surf. Sci.* **2002**, *500* (1−3), 656.
(4) Speranza, G.; Gottardi, G.; Pederzolli, C.; Lunelli, L.; Canteri, R.; Pasquardini, L.; Carli, E.; Lui, A.; Maniglio, D.; Brugnara, M.; Anderle, M. *Biomaterials* **2004**, *25*, 2029.
(5) Elbert, D. L.; Hubbell, J. A. *Annu. Rev. Mater. Sci.* **1996**, 365.
(6) (a) Langer, R. *AIChE J.* **2000**, *46*, 7, 1286. (b) Castner, D. G.; Ratner, B. D. *Surf. Sci.* **2002**, *500* (1−3), 28. (c) Schreier, S.; Malheiros, S. V. P.; de Paula, E. *Biochim. Biophys. Acta* **2000**, *1508*, 210.
(7) Claesson, P. M.; Blomberg, E.; Froberg, J. C.; Nylander, T.; Arnebrant, T. *Adv. Colloid Interface Sci.* **1995**, *57*, 161.
(8) (a) Hammer, E. L.; Tirrell, M. *Annu. Rev. Mater. Sci.* **1996**, *26*, 651. (b) Tirrell, M.; Kokkoli, E.; Biesalski, M. *Surf. Sci.* **2002**, *500* (1−3), 61.
(9) Fulzele, S. V.; Sattuwar, P. M.; Dorle, A. K. *Eur. J. Pharm. Sci.* **2003**, *20*, 53.
(10) (a) Sudesh, K.; Abe, H.; Doi, Y. *Prog. Polym. Sci.* **2000**, *25*, 1503. (b) Ha, C. S.; Cho, W. J. *Prog. Polym. Sci.* **2002**, *27*, 759.
(11) Sang, B. I.; Hori, K.; Tanji, Y.; Unno, H. *Biochem. Eng. J.* **2001**, *9*, 175.
(12) (a) Lee, S. R.; Park, H. M.; Lim, H.; Kang, T. K.; Li, X.; Cho, W. J.; Ha, C. S. *Polymer* **2002**, *43*, 8, 2495. (b) Ray, S. S.; Okamoto, M. *Macromol. Rapid Commun.* **2003**, *24*, 815.
(13) (a) Jahangir, R.; McCloskey, C. B.; McClung, W. G.; Labow, R. S.; Brash, J. L.; Santerrem, J. P. *Biomaterials* **2003**, *24*, 121. (b) Hua, A.; Chen, J.; Lun, S.; Wang, X. *Water Res.* **2003**, *37*, 4143.
(14) Nam, K.; Watanabe, J.; Ishihara, K. *Int. J. Pharm.* **2004**, *275*, 259.
(15) Acemoglu, M. *Int. J. Pharm.* **2004**, *277*, 133.
(16) (a) Davies, M. C.; Short, R. D.; Khan, M. A.; Watts, J. F.; Brown, A.; Eccles, A. J.; Humphrey, P.; Vickerman, J. C.; Vert, M. *Surf. Interface Anal.* **1989**, *14* (3), 115. (b) Davies, M. C.; Lyyn, R. A. P. *Crit. Rev. Biocompat.* **1990**, *5*, 297. (c) Davies, M. C.; Khan, M. A.; Short, R. D.; Akhtar, S.; Pouton, C.; Watts, J. F. *Biomaterials* **1990**, *11*, 228. (d) Shard, A. G.; Davies, M. C.; Li, Y. X.; Volland, C.; Kissel, T. *Macromolecules* **1997**, *30*, 3051. (e) Davies, M. C.; Lynn, R. A. P.; Langer, R.; Domb, A.; Paul, A. *Polym. Prepr. Abstr. Am. Chem. Soc.* **1990**, *31* (2), 22. (f) Shard, A. G.; Volland, C.; Davies, M. C.; Kissel, T. *Macromolecules* **1996**, *29*, 748.
(17) Pasche, S.; De Paul, S. M.; Voros, J.; Spencer, N. D.; Textor, M. *Langmuir* **2003**, *19*, 9216.
(18) Leadley, S. R.; Davies, M. C.; Vert, M.; Braud, C.; Paul, A. J.; Shard, A. G.; Watts, J. F. *Macromolecules* **1997**, *30*, 6920.
(19) Ratner, B. D. *J. Biomed. Mater. Res.* **1993**, *27*, 837.
(20) Kingshott, P.; Griesser, H. J. *Curr. Opin. Solid State Mater. Sci.* **1999**, *4*, 403.
(21) Ivanova, Tz.; Panaiotov, I.; Boury, F.; Proust, J. E.; Benoit, J. P.; Verger, R. *Colloids Surf B: Biointerfaces* **1997**, *8*, 217.
(22) Chen, X.; Shakesheff, K. M.; Davies, M. C.; Heller, J.; Roberts, C. J.; Tendler, S. J. B.; Williams, P. M. *J. Phys. Chem.* **1995**, *99*, 11537.
(23) Allen, A.; Davies, M. C.; Roberts, C. J.; Tendler, S. J. B.; Williams, P. M. *Trends Biotechnol.* **1997**, *15*, 101.
(24) Davies, M. C.; Shakesheff, K. M.; Shard, A. G.; Domb, A.; Roberts, C. J.; Tendler, S. J. B.; Williams, P. M. *Macromolecules* **1996**, *29*, 2205.
(25) Shakesheff, K. M.; Chen, X. Y.; Davies, M. C.; Domb, A.; Roberts, C. J.; Tendler, S. J. B.; Williams, P. M. *Langmuir* **1995**, *11*, 3921.
(26) Lee, J. W.; Gardell, J. A. *Macromolecules* **2001**, *34*, 3928.
(27) Luzinov, I.; Minko, S.; Tsukruk, V. V. *Prog. Polym. Sci.* **2004**, *29*, 635.
(28) Somorjai, G. A. *Chem. Rev.* **1996**, *96*, 1223.
(29) Vickerman, J. C. Ed. *Surface Analysis; The Principle Techniques*; Wiley: New York, 1997; preface.
(30) Zhuang, H. Z.; Gardella, Jr., J. A. *MRS Bull.* **1996**, *21*, 43.
(31) Losito, I.; Sabbatini, L.; Gardella, Jr., J. A. Electron, Ion, and Mass Spectroscopy. In *Comprehensive Desk Reference of Polymer Characterization and Analysis*; Brady, R. F., Jr., Ed.; Oxford University Press: New York, 2003; pp 375−407.
(32) Pireaux, J. J. *Synth. Metals* **1994**, *67* (1−3), 39.
(33) Chan, C. M.; Weng, L. T. *Rev. Chem. Eng.* **2000**, *16*, 341.
(34) Clark, D. T. In *Handbook of X-Ray and Ultraviolet Photoelectron Spectroscopy*; Briggs, D. Ed.; Heyden: London, U.K., 1977; p 211.
(35) Benninghoven, A.; Rudenauer, F. G.; Werner, H. W. *Secondary Ion Mass Spectrometry, Basic Concepts, Instrumental Aspects, Applications, and Trends*; Wiley: New York, 1987.
(36) (a) Hanton, S. D. *Chem. Rev.* **2001**, *101*, 527. (b) Vaeck, L. V.; Adriaens, A.; Gijbels, R. *Mass Spectrosc. Rev.* **1999**, *18*, 1. (c) Adriaens, A.; Vaeck, L. V.; Adams, F. *Mass Spectrosc. Rev.* **1999**, *18*, 48. (d) Werner, H. W. *Surf. Interface Anal.* **2003**, *35*, 859.
(37) (a) Gardella, Jr., J. A.; Hercules, D. M. *Anal. Chem.* **1980**, *52*, 226. (b) Li, J. X.; Johnson, Jr., R. W.; Gardella, Jr., J. A. Secondary Ion Mass Spectrometry as Applied to Thin Organic and Polymeric Films Produced by Langmuir Blodgett and Self-Assembly. In *Characterization of Organic Thin Films*; Materials Characterization Series: Surfaces, Interfaces, Thin Films of Materials 12; Ulman, A., Ed.; Manning Publications: Greenwich, CT, 1995; pp 193−212. (b) Gardella, Jr., J. A.; Wandass, J. H.; Schmitt, R. L.; Chin, R. L. Spectroscopic Analysis of Molecular Surfaces by Ion, Photoelectron and Vibrational Spectroscopy. In *Proceedings of the Second Conference on Advances in Materials Characterization*; Snyder, R. L., Ed.; Plenum: New York, 1985; pp 209−220. (d) Ibach, H.; Mills, D. L. *Electron Energy Loss Spectroscopy and Surface Vibrations*; Wiley: New York, 1982.
(38) Belu, A. M.; Graham, D. J.; Castne, D. G. *Biomaterials* **2003**, *24*, 3635.
(39) Vert, M. *Angew. Makromol. Chem.* **1989**, *166/167*, 155.
(40) Dematteis, C. I.; Davies, M. C.; Leadlty, S.; Jackson, D. E.; Beamson, G.; Briggs, D.; Heller, J.; Franson, N. M. *J. Electron. Spectrosc. Relat. Pheonm.* **1993**, *63* (3), 221.
(41) Lang, F. R.; Leonard, D.; Mathieu, H. J.; Moser, E. H.; Bertrand, P. *Macromolecules* **1998**, *31*, 6177.
(42) Veld, J. A. I.; Dijkstra, P. J.; Feijien, J. *Makromol. Chem.* **1992**, *193*, 2713.
(43) Barrera, D. A.; Zylstra, E.; Lansbury, P. T.; Langer, R. *Macromolecules* **1995**, *28*, 425.
(44) (a) Vargo, T. G.; Thompson, P. M.; Gerenser, L. J.; Valentini, R. F.; Aebischer, P.; Hook, D. J.; Gardella, J. A., Jr. *Langmuir* **1992**, *8*, 130. (b) Vargo, T. G.; Bekos, E. J.; Kim, Y. S.; Ranieri, J. P.; Bellamkonda, R.; Aebischer, P.; Margevich, D. E.; Thompson, P. M.; Bright, F. V.; Gardella, J. A., Jr. *J. Biomed. Mater. Res.* **1995**, *29*, 767. (c) Vargo, T. G.; Gardella, Jr., J. A. Modification of Surfaces Designed for Cell Growth Studies. In *Polymer Solid Interfaces*; Pireaux, J. J., Bertrand, P., Brédas, J. L., Eds.; Adam Hilger, Institute of Physics: Bristol, U.K., 1992; pp 485−494.
(45) Maulding, H. *J. Controlled Release* **1987**, *6*, 1671.
(46) Furr, B. J. A.; Hutchinson, F. G. *J. Controlled Release* **1992**, *21*, 117.
(47) Lee, W. K.; Losito, I.; Gardella, J. A.; Hicks, W. L. *Macromolecules* **2001**, *34*, 3000.
(48) Brinen, J. S.; Greenhouse, S.; Jarrett, P. K. *Surf. Interface Anal.* **1991**, *17* (5), 259.
(49) Kiss, É.; Bertóti, I.; Vargha-Butler, E. I. *J Colloid Interface Sci.* **2002**, *245*, 91.
(50) Lee, J. W.; Yu, J.; Gardella, J. A.; Hicks, W. L.; Hard, R.; Bright, F. V.; Jeong, E. D.; Lee, D. S. *Surf. Interface Anal.*, submitted for publication.
(51) Shard, A. G.; Clarke, S.; Davies, M. C. *Surf. Interface Anal.* **2002**, *33*, 528.
(52) (a) Xhou, S.; Deng, X.; Yang, H. *Biomaterials* **2003**, *24*, 3563. (b) Molpeceres, J.; Aberturas, M. R.; Guzman, M. *J. Microencapsulation* **2000**, *17* (5), 599. (c) Coombes, A. G. A.; Rizzi, S. C.; Willimason, M.; Barralet, J. E.; Downes, S.; Wallace, W. A. *Biomaterials* **2004**, *25*, 315. (d) Kim, H. W.; Knoles, J. C.; Kim, H. E. *Biomaterials* **2004**, *25*, 1279. (e) Allen, C.; Han, Y.; Maysinger, D.; Eisenberg, A *J. Controlled Release* **2000**, *63*, 275. (f) Zhu, Y. B.; Gao, C. Y.; Liu, X. Y.; Shen, J. C. *Biomacromolecules* **2002**, *3* (6), 1312. (g) Gibaud, S. A.; Awwadi, N. J.; Ducki, C.; Astier, A. *Int. J. Pharm.* **2004**, *269*, 491. (i) Vance, R. J.; Miller, D. C.; Thapa, A.; Haberstroh, K. M.; Webster, T. J. *Biomaterials* **2004**, *25*, 2095. (j) Sinha, V. R.; Bansal, K.; Kaushik, R.; Kumria, R.; Trehan, A. *Int. J. Pharm.* **2004**, *278*, 1. (k) Choi, M. J.; Biancon, S.; Andrieu, J.; Min, S. G.; Fessi, H. *Drying Technol.* **2004**, *22* (1−2), 335.
(53) (a) Cheng, Z.; Teoh, S. H. *Biomaterials* **2004**, *25*, 1991. (b) Toselli, M.; Gardella, J. A.; Messori, M.; Hawkridge, A. M.; Pilati, F.; Tonelli, C. *Polym. Int.* **2003**, *52* (8), 1262.

(54) (a) Lukyanov, A. N.; Gao, Z.; Torchilin, V. P. *J. Controlled Release* **2003**, *91*, 97. (b) Fu, J.; Fiegel, J.; Krauland, E.; Hanes, J. *Biomaterials* **2002**, *23*, 4425. (c) De Campos, A. M.; Sanchez, A.; Gref, R.; Calvo, P.; Alonso, M. J. *Eur. J. Pharm. Sci.* **2003**, *20* (1), 73. (d) Das, G. S.; Rao, C. H. R.; Wilson, R. F.; Chandy, T. *Drug Delivery* **2000**, *78* (3), 129. (e) Tansey, W.; Ke, S.; Cao, X. Y.; Pasuelo, M. J.; Walkac, S.; Li, C. *J. Controlled Release* **2004**, *94*, 29.

(55) (a) Cho, E. J.; Tao, Z.; Tang, Y.; Tehan, E. C.; Bright, F. V.; Hicks, W. L. Jr.; Gardella, Jr., J. A. *Appl. Spectro.* **2002**, *56* (11), 1385. (b) Cho, E. J.; Tao, Z.; Tang, E. C.; Tehan, E. C.; Bright, F. V.; Hicks, W. L., Jr.; Gardella, J. A., Jr. *J. Biomed. Mater. Res.* **2003**, *66A* (2), 417.

(56) Bekos, E. J.; Ranieri, J. P.; Aebischer, P.; Gardella, J. A.; Bright, F. V. *Langmuir* **1995**, *11* (3), 984.

(57) (a) Ranieri, J. P.; Bellamkonda, R.; Bekos, E. J.; Gardella, J. A.; Mathieu, H. J.; Ruiz, L.; Aebischer, P. S. *Int. J. Dev. Neruosci.* **1994**, *12* (8), 725. (b) Ranieri, J. P.; Bellamkonda, R.; Bekos, E. J.; Vargo, T. G.; Gardella, Jr., J. A.; Aebischer, P. *J. Biomed. Mater. Res.* **1995**, *29*, 779. (c) Ranieri, J. P.; Bellamkonda, R.; Jacob, J.; Vargo, T. G.; Gardella, Jr., J. A.; Aebischer, P. *J. Biomed. Mater. Res.* **1993**, *27*, 917.

(58) Degatica, N. L. H.; Jones, G. L.; Gardella, J. A. *Appl. Surf. Sci.* **1993**, *68* (1), 107.

(59) Vaelenti, R. F.; Vargo, T. G.; Gardella, J. A.; Aebischer, P. *Biomaterials* **1992**, *13* (3), 183.

(60) Pasche, S.; De Paul, S. M.; Voros, J.; Spencer, N. D.; Textor, M. *Langmuir* **2003**, *19* (22), 9216.

(61) Sabbatini, L.; Zambonin, P. G. *J. Electron. Spectrosc.* **1996**, *81* (3), 285.

(62) Kinoshita, E.; Yamkoshi, J.; Kikuchi, M. *Biosci., Biotechnol., Biochem.* **1993**, *57* (7). 1107.

(63) Sodhi, R. N. S.; Sahi, V. P.; Mittelman, V. M. *J. Electron. Spectrosc. Relat. Phenom.* **2001**, *121*, 249.

(64) Volooj, S.; Carr, C. M.; Mitchell, R.; Vickerman, J. C. *Surf. Interface Anal.* **2000**, *29*, 422.

(65) Xia, N.; Castner, D. G. *J. Biomed. Mater. Res.* **2003**, *67*A (1), 179.

(66) Arlinghaus, H. F.; Ostrop, M.; Friedrichs, O.; Feldner, J.; Gunst, U.; Lipinsky, D. *Surf. Interface Anal.* **2002**, *33*, 35.

(67) Fragu, P.; Kahn, E. *Microsc. Res. Tech.* **1997**, *36*, 296.

(68) Coullerez, G.; Lundmark, S.; Malmstrom, E.; Hult, A.; Jorg Mathieu, H. *Surf. Interface Anal.* **2003**, *35* (8), 693.

(69) Ruiz, L.; Hilborn, J. G.; Leonard, D.; Mathieu, H. J. *Biomaterials* **1998**, *19*, 987.

(70) Neff, J. A.; Tresco, P. A.; Caldwell, K. D. *Biomaterials* **1999**, *20*, 2377.

(71) Liu, X.; Fu, R. K. Y.; Poon, R. W. Y.; Chen, P.; Chu, P. K.; Ding, C. *Biomaterials* **2004**, *25*, 5575.

(72) Kingshott, P.; McArthur, S.; Thissen, H.; Caster, D. G.; Griesser, H. J. *Biomaterials* **2002**, *23*, 4775.

(73) Wagner, M. S.; Horbett, T. A.; Castner, D. G. *Biomaterials* **2003**, *24*, 1897.

(74) Barbucci, R.; Magnani, A.; Lamponi, S.; Pasqui, D.; Bryan, S. *Biomaterials* **2003**, *24*, 915.

(75) Yan, L.; Leng, Y.; Weng, L. T. *Biomaterials* **2003**, *24*, 2585.

(76) Ni, M.; Ratner, B. D. *Biomaterials* **2003**, *24*, 4323.

(77) Zhang, Z. P.; Yoo, R.; Wells, M.; Beebe, T. P. Jr.; Biran, R.; Tresco, P. *Biomaterials* **2005**, *26* (1), 47.

(78) (a) Sigurdson, L.; Carney, D. E.; Hou, Y. X.; Hall, L., III; Hard, R.; Hicks, W. L., Jr.; Gardella, J. A., Jr. *J. Biomed. Mater. Res.* **2002**, *59* (2), 357. (b) Hicks, Jr., W. L.; Sigurdson, L.; Gabalski, E.; Hard, R.; Hall, L., III; Gardella, Jr., J. A.; Powers, C.; Kumar, N.; Lwebuga-Mukasa, J. *Arch. Otolaryngol. Head Neck Surg.* **1999**, *125,* 1239. (c) Bekos, E. J.; Gardella, Jr., J. A.; Bright, F. V. *J. Inclus. Phenom. Mol. Recogn. Chem.* **1996**, *26*, 185. (d) Gardella, Jr., J. A. *A Hierarchy of Model Systems for Biomaterials Interfaces: Analysis by Electron, Ion and Vibrational Spectroscopies, Surface and Interface Analysis*; Proceedings of the Sixth European Conference on Applications of Surface and Interface Analysis; Mathieu, H. J.; Reihl, G., Briggs, D., Eds.; J. Wiley and Sons: New York, NY, 1996; pp 29−35.

(79) (a) Schamberger, P. C.; Gardella, Jr., J. A.; Grobe, G. L. III; Valint, Jr., P. L. *Polym. Prepr. Am. Chem. Soc.* **1993**, *34* (2), 58. (b) Schamberger, P. C.; Abes, J. I.; Gardella, Jr., J. A. *Colloid Surf. Part B: Biointerf.* **1994**, *3* (4), 203. (c) Schamberger, P. C.; Gardella, Jr., J. A. *Colloids Surf.* **1993**, *2* (1−3)*,* 209. (d) Schamberger, P. C.; Gardella, Jr., J. A.; Grobe, III, G. L.; Valint, Jr., P. L. *Polym. Prepr. Am. Chem. Soc.* **1992**, *33* (2), 503.

(80) (a) Valentini, R. F.; Aebischer, P.; Vargo, T. G.; Gardella, Jr., J. A. *J. Biomater. Sci., Polym. Ed.* **1993**, *5*, 13. (b) Valentini, R. F.; Vargo, T. G.; Gardella, Jr., J. A.; Aebischer, P. *Biomaterials* **1992**, *13* (3), 183.

(81) Litwiler, K. S.; Vargo, T. G.; Hook, D. J.; Gardella, Jr., J. A.; Bright, F. V. Novel Supports for the Development of High Stability Fiber Optic-Based Immunoprobes. In *Chemically Modified Surfaces*; Mottola, H. A., Steinmetz, J. R., Eds.; Elsevier Science Publishers: Amsterdam, The Netherlands, 1992; pp 307−317.

(82) Lhoest, J. B.; Wagner, M. S.; Tidwell, C. D.; Castner, D. G. *J. Biomed. Mater. Res.* **2001**, *57* (3), 432.

(83) Chen, G.; Ushida, T.; Tateishi, T. *J. Biomed. Mater. Res.* **2000**, *51* (2), 273.

(84) Coombes, A. G. A.; Rizzi, S. C.; Williamson, M.; Barralet, J. E.; Downes, S.; Wallace, W. A. *Biomaterials* **2004**, *25*, 315.

(85) Middleton, J. C.; Tipton, A. J. *Biomaterials* **2000**, *21*, 2335.

(86) Ikada, Y.; Tsuji, H. *Macromol. Rapid Commun.* **2000**, *21*, 117.

(87) (a) Göpferich, A. *Biomaterials* **1996**, *17*, 103. (b) Göpferich, A. *Macromolecules* **1997**, *30*, 2598.

(88) Williams, D. F. *Clin. Mater.* **1992**, *10*, 9.

(89) Bodmer, D.; Kissel, T.; Traechslin, E. *J. Controlled Release* **1992**, *21*, 129.

(90) St. Pierre, T.; Chiellini, E. *J. Bioact. Compat. Polym.* **1986**, *1*, 467.

(91) Tamada, J.; Langer, R. *J. Biomater. Sci., Polym. Ed.* **1992**, *3*, 315.

(92) Peppas, N. A., Langer, R. S., Eds. *Advances in Polymer Science. No. 107: Biopolymers I*; Springer-Verlag: Berlin, Germany, 1993.

(93) Schwach-Abdellaoui, K.; Heller, J.; Gurny, R. *Macromolecules* **1999**, *32*, 301.

(94) Ng, S. Y.; Vandamme, T.; Taylor, M. S.; Heller, J. *Macromolecules* **1997**, *30*, 770.

(95) Heller, J.; Himmelstein, K. J. *Methods Enzymol.* **1985**, *112*, 422.

(96) Ambrosio, A. M. A.; Allcock, H. R.; Katti, D. S.; Laurencin, C. T. *Biomaterials* **2002**, *23*, 1667.

(97) Qiu, L. Y.; Zhu, K. J. *J. Appl. Polym. Sci.* **2000**, 77, 2987.

(98) Song, S. C.; Lee, S. B.; Jin, J. I.; Sohn, Y. S. *Macromolecules* **1999**, *2188*, 8.

(99) (a) Crommen, J. H. L.; Schacht, E. H.; Mense, E. H. G. *Biomaterials* **1992**, *13*, 601. (b) Crommen, J. H. L.; Schacht, E. H.; Mense, E. H. G. *Biomaterials* **1992**, *13*, 511.

(100) Laurencin, C. T.; Koh, H. J.; Neenan, T. X.; Allcock, H. R.; Langer, R. *J. Biomed. Mater. Res.* **1987** *21*, 1231.

(101) PerezLuna, V. H.; Hooper, K. A.; Kohn, J.; Ratner, B. D. *J. Appl. Polym. Sci.* **1997**, *63* (11), 1467.

(102) Kreuter, J. *Pharm. Acta Helv.* **1983**, *58*, 217.

(103) Bender, A. R.; Von Briesen, H.; Kreuter, J.; Duncan, I. B.; Rübsamen-Waigmann, H. *Antimicrob. Agents Chemother.* **1996**, *40,* 1467.

(104) Gaspar, R.; Opperdoes, F. R.; Preat, V.; Roland, R. *Ann. Trop. Med. Parasitol.* **1992**, *86*, 41.

(105) Bodner, U. *Biotechnol. Appl. Biochem.* **1991**, *2*, 51.

(106) Chavany, C.; Trung Le, D.; Couvreuer, P.; Puisieux, F.; Hélène, C. *Pharm. Res.* **1992**, *9*, 441.

(107) Moffatt, M. F.; Cookson, W. O. C. *Nat. Med.* **1999**, *5*, 380.

(108) Roy, K.; Mao, H. Q.; Huang, S. K.; Leong, K. W. *Nat. Med.* **1999**, *5*, 387.

(109) Rhaese, S.; Briesen, H. V.; Rübsamen-Waigmann, H.; Kreuter, J.; Langer, K. *J. Controlled Release* **2003**, *92*, 199.

(110) Luo, D.; Saltzman, W. M. *Biotechnology* **2000**, *18*, 893.

(111) Cohen, H.; Levy, R. J.; Gao, J.; Fishbein, I.; Kousaev, V.; Sosnowski, S.; Slomkowski, G.; Golomb, G. *Gene Ther.* **2000**, 7, 1896.

(112) (a) Orson, F. M.; Kinsey, B. M.; Hua, P. J.; Bhogal, B. S.; Densmore, C. L.; Barry, M. A. *J. Immunol.* **2000**, *164*, 6313. (b) Orson, F. M.; Song, L.; Gautam, A.; Densmore, C. L.; Bhogal, B. S.; Kinsey, B. M. *Gene Ther.* **2002**, *9*, 463.

(113) Truong-Le, V. L.; August, J. T.; Leong, K. W. *Hum. Gene Ther.* **1998**, *9*, 1709.

(114) Brzoska, M.; Langer, K.; Coester, C.; Loitsch, S.; Wagner, T. O. F.; Mallinckrodt, C. V. *Biochem. Biophys. Res. Commun.* **2004**, *318* (2), 562.

(115) Shi, G.; Rouabhia, M.; Wang, Z.; Dao, L. H.; Zhang, Z. *Biomaterials* **2004**, *25*, 2477.

(116) Elamanchili, P.; Diwan, M.; Cao, M.; Samuel, J. *Vaccine* **2004**, *22* (19), 2406.

(117) Newman, K. D.; McBurney, M. W. *Biomaterials* **2004**, *25* (26), 5763.

(118) Mu, L.; Feng, S. S. *J. Controlled Release* **2003**, *86*, 33.

(119) Chandy, T.; Wilson, R. F.; Rao, G. H. R.; Das, G. S. *J. Biomater. Appl.* **2002**, *16* (4), 275.

(120) Shakesheff, K. M.; Evora, C.; Soriano, I.; Langer, R. *J. Colloid Interface Sci.* **1997**, *185* (2), 538.

(121) Scholes, P. D.; Coombes, A. G. A.; Illum, L.; Davis, S. S.; Watts, J. F.; Ustariz, C.; Vert, M.; Davies, M. C. *J. Controlled Release* **1999**, *59* (3), 261.

(122) (a) Zambaux, M. F.; Bonneaux, F.; Gref, R.; Alonso, M. J.; Mincent, P. Dellacherie, E.; Labrude, P.; Vigneron, C. *J. Controlled Release* **1998**, *50*, 31. (b) Zambaux, M. F.; Bonneaux, F.; Gref, R.; Dellacherie, E.; Vigneron, C. *J. Biomed. Mater. Res.* **1999**, *44* (1), 109.

(123) Yang, Y.; Chung, T. S.; Ng, N. P. *Biomaterials* **2001**, *22*, 231.

(124) Sullivan, C. O.; Birkinshaw, C. *Biomaterials* **2004**, *25*, 4375.

(125) Grassi, M.; Voinovich, D.; Moneghini, M.; Franceschinis, E.; Perissutti, B.; Filipovic-Grcic, J. *J. Controlled Release* **2003**, *88*, 381.

(126) Shakesheff, K. M.; Davies, M. C.; Heller, J.; Roberts, C. J.; Tendler, S. J. B.; Williams, P. M. *Langmuir* **1995**, *11* (7), 2547.
(127) Brindley, A.; Davies, M. C.; Watts, J. F. *J. Colloid Interface Sci.* **1995**, *171*, 150.
(128) Kostarelos, K. *Adv. Colloid Interface Sci.* **2003**, *106*, 147, and references therein.
(129) MaCarthy, S. J.; Meijs, G. F.; Mitchell, N.; Gunatillake, A. P.; Heath, G.; Brandwood, A.; Schindhelm, K. *Biomaterials* **1997**, *18*, 1387.
(130) Schbert, M. A.; Wiggins, M. J.; Schaefer, M. P.; Hitner, A.; Anderson, J. M. *J. Biomed. Mater. Res.* **1995**, *29*, 337.
(131) Fredericks, R. J.; Melveger, A. J.; Dolegiewitz, L. J. *J. Polym. Sci., Polym. Phys. Ed.* **1984**, *22*, 57.
(132) Scott, G.; Gilead, D. *Degradable Polymers*; Chapman & Hall: London, U.K., 1995.
(133) Lee, W. K.; Iwata, T.; Abe, H.; Doi, Y. *Macromolecules* **2000**, *33*, 9535.
(134) Lee, W. K.; Gardella, Jr., J. A. *Langmuir* **2000**, *16*, 3401.
(135) Lee, W. K.; Cho, W. J.; Ha, C. S.; Takahara, A.; Kajiyama, T. *Polymer* **1995**, *36*, 1229.
(136) Ha, C. S.; Lee, W. K.; Kim, I. In *Natural Polymers*; PBM Series 3; Williams, P. A., Ed.; Citus Books: London, U.K., 2005; in press.
(137) Lee, W. K.; Doi, Y.; Ha, C. S. *Macromol. Biosci.* **2001**, *1*, 114.
(138) Lee, W. K.; Ryou, J. H.; Ha, C. S. *Surf. Sci.* **2003**, *542*, 235.
(139) Chu, C. C. *Polymer* **1985***, 26*, 591.
(140) Ryou, J. H.; Ha, C. S.; Kim, J. W.; Lee, W. K. *Macromol. Biosci.* **2003**, *3*, 44.
(141) Gardella, Jr., J. A.; Novak, R. F.; Hercules, D. M. *Anal. Chem.* **1984**, *56*, 6 (8), 1371.
(142) Lee, J. W.; Gardella, J. A. *Am. Soc. Mass Spectrosc.* **2002**, *13*, 1108.
(143) Erbil, Y. H.; Yasar, B.; Suzer, S.; Baysal, B. M. *Langmuir* **1997**, *13*, 5484.
(144) Zhang, H.; Ward, I. M. *Macromolecules* **1995**, *28*, 7622.
(145) Koyama, N.; Doi, Y. *Macromolecules* **1996**, *29*, 5843.
(146) Li, Y.; Volland, C.; Kissel, T. *Polymer* **1998**, *39*, 3087.
(147) (a) Chen, J.; Gardella, Jr., J. A. *Macromolecules* **1999**, *32*, 7380. (b) Lee, J. W.; Gardella, J. A. *Anal. Bioanal. Chem.* **2002**, *373* (7), 526.
(148) Frazza, E. J.; Schimitt, E. E. *J. Biomed. Mater. Res. Symp.* **1971**, *1*, 43.
(149) Chujo, K.; Kobayashi, H.; Suzuki, J.; Tokuhara, S. *Makromol. Chem.* **1967**, *100*, 267.
(150) Chatani, Y.; Suehiro, K.; Okita, Y.; Tadokoro, H.; Chujo, K. *Makromol. Chem.* **1968**, *113*, 215.
(151) Gilding, D. K.; Reed, A. M. *Polymer* **1979**, *20*, 1459.
(152) Chujo, K.; Kobayashi, H.; Tokuhara, S.; Tanabe, M. *Makromol. Chem.* **1967**, *100*, 262.
(153) Hirano, H.; Wsai, T.; Saegusa, T.; Furukawa, J. *J. Chem. Soc. Jpn.* **1964**, *67*, 604.
(154) Kenley, R. A.; Lee, M. O.; Mahoney II, T. R.; Sanders, L. M. *Macromolecules* **1987**, *20*, 2398
(155) Pitt, C. G.; Schindler, A. In *Controlled Drug Delivery*; Bruck, S. D., Ed.; CRC Press: Boca Raton, FL, 1983.
(156) Leenslag, J. W.; Pennings, A. J.; Bos, R. R. M.; Rozema, F. R.; Boering, G. *Biomaterials* **1987**, *8*, 311.
(157) Kulkarni, R. K.; Pani, K. C.; Neuman, C.; Leonard, F. *J. Biomed. Mater. Res.* **1971**, *5*, 169.
(158) Miller, R. A.; Brady, J. M.; Cutright, D. E. *J. Biomed. Res.* **1977**, *11*, 711.
(159) Jackanicz, T. M.; Nash, H. A.; Wise, D. L.; Gregory, J. *Contraception* **1973**, *8*, 227.
(160) Anderson, L. C.; Wise, D. L.; Howes, J. F. *Contraception* **1976**, *13*, 375.
(161) Wise, D. L.; McCormick, G. J.; Willet, G. P.; Anderson, L. C. *Life Sci.* **1976**, *19*, 867.
(162) Getter, L. Presented at the Fourth Annual Biomaterials Symposium, Clemson University, 1972.
(163) Schmitt, E. E; Polistina, R. A. U.S. Patent 3297033, 1967.
(164) Schmitt, E. E.; Epstein, M.; Polistina, R. A. U.S. Patent 3422871, 1969.
(165) Glick, A. U.S. Patent 3626948, 1971.
(166) Vainionpaa, S.; Rokkanen, P.; Tormala, P. *Prog. Polym. Sci.* **1989**, *14*, 679.
(167) Williams, D. F. *J. Mater. Sci.* **1982**, *17*, 1233.
(168) *Controlled Release of Biologically Active Agents*; Baker, R. W., Ed.; Wiley: New York, 1987.
(169) Cooke, T. F. *J. Polym. Eng.* **1990**, *9*, 171.
(170) Reed, A. M.; Gilding, D. K. *Polymer* **1981**, *22*, 494.
(171) Pitt, C. G. In *Biodegradable Polymers and Plastics*; Vert, M., Feijen, J., Albertsson, A., Scott, G., Chiellini, E., Eds.; Royal Society of Chemistry: Cambridge, U.K., 1992.
(172) Chu, C. C. *J. Biomed. Mater. Res.* **1981**, *15*, 795.
(173) Ginde, R. M.S. Thesis, State University of New York at Buffalo, 1985.

(174) Chen, J. X.; Lee, J. W.; de Gatica, N. L. H.; Burkhardt, C. A.; Hercules, D. M.; Gardella, J. A. *Macromolecules* **2000**, *33* (13), 4726.
(175) Lewis, D. H. Controlled release of bioactive agents from lactide/glycolide polymers. In *Biodegradable Polymers as Drug Delivery Systems*; Chasin, M., Langer, R., Eds.; Dekker: New York, 1990; pp 1–41.
(176) (a) Pitt, C. G.; Gratzel, M. M.; Kimmel, G. L.; Surles, J.; Schindler, A. *Biomaterials* **1981**, *2*, 215. (b) Makino, K.; Pjsjo, A. H.; Kondo, T. *J. Microencapsulation* **1986**, *3*, 203.
(177) (a) Li, S. M.; Carreau, H.; Vert, M. *J. Mater. Sci. Med.* **1990**, *1*, 123. (b) Li, S. M.; Carreau, H.; Vert, M. *J. Mater. Sci. Med.* **1990**, *1*, 131. (c) Therin, M.; Christel, P.; Li, S. M.; Carreau, H.; Vert, M. *Biomaterials* **1992**, *13*, 594.
(178) (a) Klompmaker, J.; Jansen, H. W. B.; Verth, R. P. H.; deGroot, J. H.; Nijenhuis, A. J.; Pennings, A. J. *Biomaterials* **1991**, *12*, 810. (b) Bostman, O. M. *Clin. Orthop. Relat. Res.* **1992**, *278*, 193.
(179) (a) Tu, C.; Cai, Q.; Yang, J.; Wan, Y.; Bei, J.; Wang, S. *Polym. Adv. Technol.* **2003**, *14*, 565. (b) Kim, B. S. *Trends Biotechnol.* **1998**, *16*, 224.
(180) Langer, R.; Vacanti, J. P. *Tissue Eng. Sci.* **1993**, *260*, 920.
(181) (a) Berkland, C.; Kipper, M. J.; Barasimhan, B.; Kim, K.; Pack, D. W. *J. Controlled Release* **2004**, *94*, 129. (b) Leadley, S. R.; Shakesheff, K. M.; Davies, M. C.; Heller, J.; Franson, N. M.; Paul, A. J.; Brown, A. M.; Watts, J. F. *Biomaterials* **1998**, *19* (15), 1353. (c) Gander, B.; Meinel, M.; Walter, E.; Merkle, H. P. *Chimia* **2001**, *55*, 212. (d) Ignatius, A. A.; Claes, L. E. *Biomaterials* **1996**, *17*, 831. Waeckerle-Men, Y.; Scadenlla, E.; Allmen, E. U.; Ludewig, B.; Gillessen, S.; Merkle, H. P.; Gander, B.; Groettrup, M. *J. Immunol. Methods* **2004**, *287*, 109. (e) Chen, G.; Sato, T.; Ushida, T.; Hirochika, R.; Tateishi, T. *FEBS Lett.* **2003**, *542* (1–3), 95. (f) Waeckerle-Men, Y.; Scadenlla, E.; Allmen, E. U.; Ludewig, B.; Gillessen, S.; Merkle, H. P.; Gander, B.; Groettrup, M. *J. Immunol. Methods* **2004**, *287*, 109.
(182) (a) Okada, H.; Toguchi, H. *Crit. Rev. Ther. Drug Carrier Syst.* **1995**, *12*, 1. (b) Jain, R.; Shah, N. H.; Malick, A. W.; Rhodes, C. T. *Drug Dev. Ind. Pharm.* **1998**, *24*, 703. (c) Govender, T.; Stolnik, S.; Garnett, M. C.; Illum, L.; Davis, S. S. *J. Controlled Release* **1999**, *57*, 171. (d) Takada, H.; Uda, Y.; Toguchi, H.; Ogawa, Y. *PDA J. Pharm. Sci. Technol.* **1995**, *49*, 180.
(183) (a) Perugini, P.; Genta, I.; Conti, B.; Modena, T.; Pavanetto, F. *AAPS Pharm. Sci. Technol.* **2001**, *2* (Article 10). (b) Blanco-Prieto, M. J.; Fattal, E.; Gulik, A.; Dedieu, J. C.; Roques, B. P.; Couvreur, P. *J. Controlled Release* **1997**, *43*, 81. (c) Fu, K.; Pack, D. W.; Klibanov, A. M.; Langer, R. *Pharm. Res.* **2000**, *17*, 100.
(184) Wang, L.; Chaw, C. S.; Yang, Y. Y.; Moochhala, S. M.; Zhao, B.; Ng, S.; Heller, J. *Biomaterials* **2004**, *25*, 3275.
(185) Dauner, M.; Muller, E.; Wagner, B.; Planck, H. In *Proceedings of 4th International Conference on Degradation Phenomena on Polymeric Materials*; Planck, H., Dauner, M., Renardy, M., Eds.; Springer-Verlag: Berlin, Germany. 1992.
(186) Li, S. M.; Vert, M. *Macromolecules* **1994**, *27*, 3107.
(187) Allen, A.; Davies, M. C.; Roberts, C. J.; Tendler, S. J. B.; Williams, P. M. *Trends Biotechnol.* **1997**, *15*, 101.
(188) Lambeek, G.; Vorenkamp, E. J.; Schouten, A. J. *Macromolecules* **1995**, *28*, 2023.
(189) Vila, N.; Minones, J.; Iribarnegaray, E.; Conde, O.; Casas, M. *Colloid Polym. Sci.* **1997**, *275*, 580.
(190) Ivanova, T.; Panaiotov, I.; Boury, F.; Benoit, J. P.; Verger, R. *Colloids Surf., B* **1997**, *8*, 217.
(191) Iwata, T.; Doi, Y. *Macromolecules* **1998**, *31*, 2461
(192) Lee, W. K.; Gardella, J. A. *Langmuir* **2000**, *16*, 3401.
(193) Lee, W. K.; Nowak, R. W.; Gardella, J. A. *Langmuir* **2002**, *18*, 2309.
(194) Cha, Y.; Pitt, G. G. *Biomaterials* **1990**, *11*, 108.
(195) Kumagai, Y.; Doi, Y. *Biomaterials* **1992**, *36*, 241.
(196) (a) Jignani, M.; Merkli, A.; Sintzel, M. B.; Bernatchez, S. F.; Kloeti, W.; Heller, J.; Tabatabay, C.; Gurny, R. *J. Controlled Release* **1997***, 48*, 115. (b) Weinhold, A.; Abdellaoui, K. S.; Barr, J.; Ng, S.; Shen, H. R.; Gurny, R.; Heller, J. *J. Controlled Release* **2001**, *71*, 31. (c) Sintzel, M. B.; Heller, J.; Ng, S. Y.; Tabatabay, C.; Abdellaoui, K. S.; Gurny, R. *J. Controlled Release* **1998**, *55*, 213. (d) Heller, J. *Adv. Polym. Sci.* **1993**, *107*, 41. (e) Ng, S. Y.; Vandamme, T.; Taylor, M. S.; Heller, J. *Macromolecules* **1997**, *30*, 770. (f) Ng, Y.; Shen, H. R.; Lopez, E.; Zherebin, Y.; Barr, J.; Schacht, E.; Heller, J. *J. Controlled Release* **2000**, *65*, 367. (g) Yang, Y.; Wan, J. P.; Chung, T. S.; Pallathadka, P. K.; Ng, S.; Heller, J. *J. Controlled Release* **2001**, *75*, 115. (h) Wan, P.; Yang, Y. Y.; Chung, T. S.; Tan, D.; Ng, S.; Heller, J. *J. Controlled Release* **2001**, *75*, 129.
(197) Shah, S. S.; Cha, Y.; Pitt, C.G. *J. Controlled Release* **1992***, 18*, 261.
(198) (a) Alonso, M. J.; Cohen, S.; Park, T. G.; Gupta, R. K.; Siber, G. R.; Langer, R. *Pharm. Res.* **1993**, *10*, 945. (b) Cohen, S.; Yoshioka, T.; Lucarelli, M.; Hwang, L. H.; Langer, R. *Pharm. Res.* **1991**, *8*, 713.

(199) Wang, J.; Wang, B. M.; Schwendeman, S. P. *Biomaterials* **2004**, *25*, 1919.
(200) Lee, J. W.; Gardella, Jr., J. A.; Hicks, Jr., W.; Hard, R.; Bright, F. V. *Pharm. Res.* **2003***, 20* (2), 149.
(201) Morrison, R. T.; Boyd, R. N. *Organic Chemistry*, 5th ed.; Allyn and Bacon: Boston, MA, 1987; p 934.
(202) Chen, J. X.; Hernandez de Gatica, N. L.; Lee, J. W.; Gardella, Jr., J. A. U.S. Patent 6,670,190 B2 (Awarded December 30, 2003).
(203) Lee, J. W.; Gardella, J. A. *Anal. Chem.* **2003**, *75*, 2950.
(204) Lee, J. W.; Gardella, J. A. *Appl. Surf. Sci.* **2004**, *231−2*, 442.

(205) (a) Gillen, G.; Roberson, S. *Rapid Commun. Mass Spectrom.* **1998**, *12*, 1303. (b) Kotter, F.; Benninghoven, A. *Appl. Surf. Sci.* **1998**, *133*, 47. (c) Appelhans, A. D.; Delmore, J. *Anal. Chem.* **1989**, *61*, 1087. (d) Gillen, G.; King, R. L.; Chmara, F. *J. Vac. Sci. Technol. A* **1999**, *17* (3), 845.
(206) Mahoney, C. M.; Roberson, S.; Gillen, G. *Appl. Surf. Sci.* **2004**, *231−2*, 174.
(207) Church, S.; Harris, S. J.; Rattana, A.; Watts, J. F. *Surf. Interface Anal.* **2002**, *34*, 19.